1989

The synthesis and characterization of some tungsten nitrides and reduced molybdenum oxides

Clark Dale Carlson
Iowa State University

Order Number 9014887

The synthesis and characterization of some tungsten nitrides and reduced molybdenum oxides

Carlson, Clark Dale, Ph.D.

Iowa State University, 1989

U·M·I
300 N. Zeeb Rd.
Ann Arbor, MI 48106

The synthesis and characterization of some tungsten nitrides and reduced molybdenum oxides

by

Clark Dale Carlson

A Dissertation Submitted to the

Graduate Faculty in Partial Fulfillment of the

Requirements for the Degree of

DOCTOR OF PHILOSOPHY

Department: Chemistry
Major: Inorganic Chemistry

Approved:

Signature was redacted for privacy.

In Charge of Major Work

Signature was redacted for privacy.

For the Major Department

Signature was redacted for privacy.

For the Graduate College

Iowa State University
Ames, Iowa

1989

TABLE OF CONTENTS

LISTS OF TABLES

LISTS OF FIGURES

GENERAL INTRODUCTION

Molybdenum and tungsten compounds have been the subject of much research since the discovery of the elements. The applications of these compounds varies widely from use in the alloying of steels[1] and as refractory materials (e.g., WC for cutting tools and Mo_2Si for resistance heaters) to the iron-molybdenum cofactor in nitrogenase and endogenous tungsten in bacterial enzymes[2]. The many applications and uses of molybdenum and tungsten materials and their relative availability (1.2 ppm in the earth's crust) makes them ideal candidates for scientific inquiry. This thesis shall deal with three areas of research on the chemistry of these two elements.

Studies of the alkoxides of tungsten and molybdenum[3] have led to the discovery of a large number of compounds which contain metal cluster units that exhibit metal-metal bonding. Besides the very fascinating chemistry which these compounds exhibit, alkoxides are thought of as precursors to metal oxide ceramics[4]. The decomposition (thermal and hydrolytic) of alkoxides has been used as a route to the preparation of high purity ceramics via particles with higher surface area than those made using conventional high temperature processing. This chemistry has given impetus to the study of using other materials as precursors to different ceramics. The use of

amido, nitrido, and azido groups as possible precursors for nitrides has been undertaken.

A second area of research that has seen a great deal of activity is the study of reduced oxides of molybdenum due to the discovery of $NaMo_4O_6$[5]. Many of these reduced oxides contain infinite chains of edge-shared molybdenum octahedra, such as $NaMo_4O_6$, $Sc_{0.75}Zn_{1.25}Mo_4O_7$[6], $Ca_{5.45}Mo_{18}O_{32}$[7], and $Gd_4Mo_4O_{11}$[8]. Many other structure types have been observed as well, including the Hollandite structure of $Ba_{1.14}Mo_8O_{16}$[9], the orthogonal nonintersecting molybdenum octahedral chains in $LiMo_8O_{10}$[10] and the fused rhomboidal clusters in Na_xMoO_2[11]. Recently, some discrete molybdenum condensed octahedral cluster species have been observed in the compounds $In_{11}Mo_{40}O_{62}$[12], $NdMo_8O_{14}$[13], $La_2Mo_{10}O_{16}$[14]. An in-depth study of some of the physical properties of the compound $NdMo_8O_{14}$ and its analogues has provided some interesting results regarding the electronic behavior of the cluster species. The preparation of the analogues also proved to be quite challenging.

The final area of interest was the preparation and single crystal x-ray structure of an iron - nickel - molybdenum intermetallic compound. This species was observed in a high temperature reaction mixture containing oxygen. While the phase , $Ni_xFe_{7-x}Mo_6$, has been observed, the growth of

single crystals has proven highly difficult and only twinned crystals had previously been observed.

Explanation of Dissertation Format

This dissertation consists of three sections which are written in a form suitable for publication in a technical journal. Although references cited in the general introduction are found at the end of the dissertation, each section contains an independent listing of references and notes which are cited in that section.

Section I

SYNTHESIS OF NITRIDE PRECURSORS

INTRODUCTION

Ceramic materials have been used throughout history for various purposes, from pottery in ancient times to refractory materials in high temperature structural applications in modern times. Most ceramic materials are prepared using techniques which involve extremes in temperature and/or pressure. Of late, there has been an increasing focus on the preparation of high temperature ceramic materials using molecular precursors[1]. In these methods, molecular compounds containing the necessary components (e.g., a metal and oxygen) are prepared at low temperatures and are then further processed at temperatures below those normally used to obtain the desired ceramic material. The advantages of a low temperature synthetic route are manifold. In the case of catalytic materials, a low temperature synthesis will provide finely divided materials with high surface area and greater reactivity. Another advantage is the possibility of obtaining metastable phases with interesting and unique properties which may not be thermodynamically possible in high temperature preparations. There is also the added bonus of reduced energy costs when using lower temperatures.

The purpose of this investigation was to prepare and study tungsten and molybdenum nitrides and nitride precursors using low temperature methods.

Review of Nitrides

The nitrides of tungsten and molybdenum have been studied for a number of years for a variety of reasons. Some of the earliest studies were on the preparation of the nitrides of tungsten and molybdenum with ammonia at high temperatures[2], since these metals are used as catalysts in the preparation of ammonia. Langmuir[3] studied the effect of using nitrogen in tungsten filament lamps. He found that the brown powdery film on the inner surface of the lamps was a nitride formed when vaporization of tungsten occurred, which he purported to be WN_2. Iwana *et al.*[4] did a study on the preparation of several transition metal nitrides for use as self aligned gates in electronic components. The study showed two mechanisms for nitride formation, viz. by surface nitridation and vapor phase reaction, the latter being the route of formation of the tungsten nitride W_2N, with no higher oxidation state nitrides being observed.

A number of research groups have performed studies on the preparation of nitrides as thin film substrates. In early work by Pinsker and Khitrova[5] and Gunther and Schneider[6], the preparations of a number of nitride phases WN_x are reported where $0.5 \leq x \leq 2$. These nitrides were formed by passing ammonia over previously deposited thin films of tungsten at temperatures

greater than 750°C. The samples were then cooled rapidly. Various hexagonal and cubic species, characterized by electron diffraction, were obtained in this fashion with several compound present on each film where the thickness of the tungsten layer influencing what nitride was formed in addition to the reaction conditions. Later thin film preparations by different groups[7] showed that only WN_x species where $x \leq 1$ were formed. In the earlier experiments, the quenching of the materials could have caused some disorder in the system, giving two sites which perhaps are only partially occupied. An indication of this was the close approach of nitrogen atoms, 1.71 Å, in the case of WN_2. Recently, the thin film studies have focused on the use of nitrides of tungsten and molybdenum for low resistance contacts to GaAs semiconductors[8]. These species consisted of the lower oxidation state nitrides such as W_2N and Mo_2N. Other methods of preparation have included reactive sputtering and ion implantation[9], nitrogen plasma reactions[10], and reactions of the metals with hydrogen cyanide gas[11]. In all of these cases involving high temperature preparations, the only nitrides observed have had the metals in the oxidation state of +3 or less. Schonberg [12] has also performed extensive studies on the nitrides of tungsten and molybdenum. In these studies, again only the lower oxidation state species were observed. For molybdenum nitrides the compounds have been given the designations α, for molybdenum with very little dissolved nitrogen; β, for

Mo_3N; γ, for FCC Mo_2N and δ for hexagonal MoN. For the tungsten nitrides the designations are α, for tungsten with very little dissolved nitrogen; β, for W_3N; γ for W_2N; and δ for WN with the tungsten carbide structure. WN (B1 structure type) with the rock salt structure has also been observed.

A possible explanation for the dearth of information about the higher oxidation state nitrides is described in thermodynamic and kinetic studies by Lyutaya[13] and Lakhtin *et al.*[14]. The experiments show that with increasing temperature, ΔG_f° for the Mo_2N decreases, making it the more favorable compound at higher temperatures instead of the higher nitrides. They observed that the reaction of the tungsten metal with ammonia at 600°C gave the product W_2N which started to decompose to the elements at 800°C. From the data presented, it appeared that the lower oxidation state materials are more stable at the higher temperatures.

A great deal of activity has been expended on the compound MoN (B1 structure type) and its tungsten analogue since Boyer *et al.*[15] performed calculations which indicated that the former might be a high T_c superconductor. These compounds have the rock salt structure and are formed under high pressure. Further work[16] has shown that B1-MoN has a T_c as high as 14.9 K or as low as 3 K, depending on the researchers and the method of preparation, which range from ammonolysis to reactive sputtering in a nitrogen atmosphere.

While much research has been instigated to find precursors for silicon nitrides, very little emphasis has been placed on finding other routes to the nitrides of molybdenum and tungsten. This study was undertaken to expand the knowledge in this area.

MATERIALS AND METHODS

All of the air and moisture sensitive materials in this study were manipulated using vacuum and Schlenk line techniques and an inert atmosphere glove box. The impurities in the molybdenum pentachloride and tungsten hexachloride (Pressure Chemicals) were removed by sublimation. The hexamethyldisilane, trimethylsilylazide, lithium bis(trimethylsilyl)amide and sodium amide were used as obtained from Aldrich Chemical Co. The ammonia was condensed on to freshly cut sodium metal and distilled to remove any impurities. All of the solvents were dried and deoxygenated prior to use.

Synthesis of Starting Materials

MNCl3 (M = Mo or W)

The nitride trichlorides of molybdenum and tungsten were first prepared By Dehnicke and Strahle[17] in the following manner:

$$MoCl_5 + ClN_3 \longrightarrow MoNCl_3 + N_2\uparrow + 3/2\ Cl_2\uparrow \quad (1)$$

$$WCl_6 + ClN_3 \longrightarrow Cl_2\uparrow + W(N_3)Cl_5 \longrightarrow WNCl_3 + N_2\uparrow + Cl_2\uparrow \quad (2)$$

A slight modification was made in the preparation of the nitride trichlorides used in this study. The source of azide was trimethylsilylazide (TMSA), a much more convenient reagent to handle, which gives trimethylsilylchloride as an easily removed byproduct. Dichloroethane was used as the solvent owing to the suspected carcinogenic nature of carbon tetrachloride. The preparation of $MoNCl_3$ was identical to the previously stated case except as noted above, with the product formed immediately upon addition of the TMSA. The product was filtered and purified by sublimation. The preparation of $WNCl_3$ was a little more difficult in that the tungsten azide chloride appears to be stable in solution. The azide chloride formed will decompose to $WNCl_3$ upon standing as a solid at room temperature for several days. Anal. Calculated Cl for $MoNCl_3$: 49.17%. Found: 49.10%. Calculated Cl for $WNCl_3$: 34.96%. Found: 34.88% The compounds were also identified by their characteristic bands in the IR spectra, 1045 cm^{-1} for ν (Mo≡N) and 1085 cm^{-1} for ν (W≡N).

γ-$MoCl_2$

The γ-$MoCl_2$ was prepared by the thermal degradation of $[Mo(CO)_4Cl_2]_2$. The compound was prepared according to the procedure reported by Holste and Schafer[18]:

$$2Mo(CO)_6 + 2Cl_{2(l)} \longrightarrow [Mo(CO)_4Cl_2]_2 + 4CO \qquad (3)$$

The yellow $[Mo(CO)_4Cl_2]_2$ is then heated in a dynamic vacuum while the temperature is slowly raised to 100°C in order to drive off the carbon monoxide. Anal. Calculated Cl: 42.47%. Found:42.50%. The IR spectrum showed bands only in the metal chlorine range, < 450 cm^{-1}.

Analytical Procedures

Molybdenum and tungsten analysis

Molybdenum and tungsten were determined gravimetrically as the trioxides. The conversion to the oxides was accomplished via addition of oxidizing solutions, either nitric acid or ammonium hydroxide and hydrogen peroxide, to a weighed sample in a tared crucible. The solutions were slowly evaporated to dryness and then ignited in a muffle furnace. Ignition temperatures were 500°C for MoO_3 and 800°C for WO_3 to insure complete combustion[19] without loss of MO_3 by vaporization.

Chlorine analysis

Samples for chlorine analysis were hydrolyzed in hot KOH or NH_4OH solutions with addition of H_2O_2. The samples were then heated to boiling to drive off excess H_2O_2 and then made slightly acidic with dilute nitric acid. The resulting solutions were then potentiometrically titrated with a standardized silver nitrate solution.

Oxidation state analysis

Oxidation state determinations for molybdenum and tungsten were performed by use of a cerium(IV)ammonium sulfate solution which was prepared and standardized according to standard procedures[20]. Each sample was dissolved in a known volume of the standard Ce(IV) solution. Some samples required heating for complete dissolution. A known quantity of Fe(II) solution[21] was then added to react with the excess Ce(IV). The excess Fe(II) was then back titrated with more Ce(IV) solution to determine the quantity of Ce(IV) used to oxidize the sample. The end point was determined potentiometrically with a calomel reference electrode and a platinum indicating electrode.

Physical Methods

X-ray powder diffraction

Routine x-ray powder patterns were obtained on a Enraf Nonius Delft triple focusing Guinier camera using Cu $K\alpha_1$ radiation ($\lambda = 1.54046$ Å). The x-ray powder data used in the Reitveld refinement of $W(NH)_3$ was obtained on a Phillips ADP3520 X-ray powder camera using Cu radiation.

Infrared spectrocopy

Infrared spectra were recorded using an IBM IR/90 Fourier Transform infrared spectrometer. Samples were prepared as Nujol mulls and pressed between cesium iodide plates. The samples were taken to the spectrometer in nitrogen filled jars and quickly transferred to the nitrogen filled sample chamber to minimize the possibility of exposure to air or moisture. The spectra were recorded separately for the mid-IR (4000 - 600 cm^{-1}) and far IR (600 - 200 cm^{-1}).

Thermogravimetric analysis

Thermogravimetric analyses were performed on a Cahn System 113 Thermogravimetric Analyzer. All experiments were run on samples which weighed between 9.00 and 10.00 milligrams. In the experiments run under flowing argon, the system was flushed with argon for approximately twelve hours prior to each run, however, due to design flaws, a small amount of oxygen remained in the system causing slight oxidation of some of the samples at higher temperatures. Oxidation experiments were performed in air under static conditions.

Solid state nuclear magnetic resonance

The solid state NMR spectrum was measured by Vinko Rutar in the Iowa State Instrument Services Group on a Bruker MSL-300 Solid State NMR spectrometer. The conditions used in the experiment were a resonance frequency of 300 MHz in a field of 8 Tesla with a rotation frequency of 3924 per second and a pulse width of 1.500 μsec.

RESULTS AND DISCUSSION

In the preparation of nitrides using low temperature methods, a number of problems had to be considered. The choice of starting materials was of great importance. The use of the chlorides as the source of molybdenum and tungsten was based on the reactivity of these compounds, their solubility in numerous solvents and their availability.

The choice of sources for the nitrogen component involved a few more considerations. The ideal case would involve compounds which would leave only nitrogen coordinated to the metal, e.g., the compound $MoN(N_3)_3py_2$[22]. However, the latter compound has been isolated and, as would be expected, it is very explosive. An attempt was made to perform a controlled decomposition in refluxing chlorobenzene on the compound $MoN(N_3)Cl_2$, but evidently the temperature was not high enough to cause the loss of the nitrogen and chlorine. The azide subsequently was isolated and proved to be shock sensitive. The next best situation would be to have only nitride, imide or amide groups bound to the metal. For these experiments, the desired compounds were prepared from the reaction of the nitride chloride with metal amides and ammonia. The materials prepared by using this approach were the most promising and will be discussed herein.

Another possibility would be the use of organic or organosilyl amines or amides as the nitrogen source. A possible problem with this sort of approach would be that there are many more elements present that can form binary compounds with the metals and, since molybdenum and tungsten form a number of extremely stable carbides and silicides, the organic groups must be labile enough to be removed during the processing to the nitrides. Some silyl containing compounds were used both as sources of nitrogen and as reducing agents and/or chlorine getters. The use of silyl groups had the advantage that the silicon chlorine bond is strong and the formation of that bond in Me_3SiCl would facilitate the removal of chlorine from the system.

The choice of solvents could also adversely affect the final products. Strongly coordinating solvents could remain attached to the precursor during the final processing to the ceramic, again making the formation of a carbide or mixed carbide-nitride a possibility. For this reason, as well as the increased solubility of the reactants, chlorocarbons and ammonia were the main solvents used. A few experiments were also carried out in tetrahydrofuran and acetonitrile in an attempt to solubilize intermediates and facilitate the removal of chlorine from the compounds.

The final stage in the process would be to prepare the nitrides by reacting the precursors to remove all nonessential components. Several reactions of the precursors were carried out in vacuum, static and dynamic,

and in various gases (Ar, N_2, and NH_3), both flowing and at static pressures. The following sections will describe the processing done first in the molybdenum chemistry and then in the more successful tungsten chemistry.

Molybdenum Chemistry

In the preparation of nitride precursors for molybdenum, the starting materials were γ-$MoCl_2$ and $MoNCl_3$. The $MoNCl_3$ already contains both the metal and the nitrogen with a triple bond and the metal is in its highest oxidation state, +6. The Mo≡N bond is easy to identify in the IR with a frequency at 1045 cm^{-1} and can be followed throughout the various steps performed to remove or replace the chlorines. In the case of γ-$MoCl_2$ the nitrogen atoms must be added and the molybdenum must be oxidized. A reason for using the γ-$MoCl_2$ is its high reactivity.

The next step in the process was to either remove the remaining chlorines or replace them with other nitrogen containing species. The final step would then be to transform the molecular species into the nitride, by pyrolysis or further reaction in a static or flowing gas (e.g., Ar, N_2, NH_3). This part of the dissertation will describe the reactions studied for the preparation of the nitride precursors of molybdenum.

It was considered that the best approach for conversion of γ-$MoCl_2$ would be to react it with trimethylsilylazide (TMSA) to form $Mo(N_3)Cl$; then nitrogen could be evolved to give the nitride monochloride without isolating the azide, since azides are usually highly unstable. This reaction was performed in various solvents as well as in various stoichiometries. Choice of the solvent was made based on boiling point since sufficient energy to split off the nitrogen while oxidizing the molybdenum was necessary in the reaction. Regardless of the quantity of TMSA and the solvent used (dichloromethane, dichloroethane, chlorobenzene, acetonitrile), the products of the reactions were the same:

$$\gamma\text{-}MoCl_2 + (CH_3)_3SiN_3 \longrightarrow Mo(N_3)Cl + (CH_3)_3SiCl \qquad (4)$$

The product of the reaction was a dark brown powder, similar to the starting material, which came out of solution quickly upon addition of the TMSA. The product was then filtered and washed with the reaction solvent to provide a dark brown solid. When THF was used as the solvent, the compound remained in solution and was isolated by stripping off the solvent after filtration, and also gave a dark brown solid. These solids were shock tested to determine if they were explosive, and were found to be passive. The IR spectra of the products from non-coordinating solvents showed the

following bands: 2110, 2070, and 1987 cm^{-1} (ν N-N); 1095 cm^{-1}, (ν N-N); 594 cm^{-1} (δ NNN); and 360 cm^{-1} (ν Mo-Cl). From these data it appears that the compound is an azide with chlorine atoms still attached. The product isolated from THF had a similar IR spectrum with the bands of coordinating THF present as well. Anal. Calculated for $Mo(N_3)Cl$: Mo, 55.3%; Cl, 20.44%; oxidation state, +2. Found: Mo, 55.0%; Cl, 20.53%; oxidation state, +1.9. The chlorine to molybdenum ratio found was 1:1, which is what was expected for $Mo(N_3)Cl$. The objective of obtaining a molybdenum nitrogen species was realized however, there was still chlorine in the product and the oxidation state remained very low. Further reactions of the product were undertaken in an attempt to make a nitride form this azido compound. Heating to 150°C in a dynamic vacuum did not appear to change the product because both Mo-Cl and azide frequencies were still present in the IR spectrum. The chlorine to molybdenum ratio of this compound was still 1:1 with only slightly higher percentages of each at 21.45% Cl and Mo 55.7%. The methods used to replace and/or remove all of the chlorine from these compounds to form the nitrides have been proven inadequate. More vigorous methods will have to be attempted which may be hazardous due to the nature of heavy metal azides.

In using the trichloronitridomolybdenum(VI) species, half of the problem of producing MoN_2 was already solved. The Mo≡N bond is very strong and

its presence in compounds is readily identifiable by its IR stretch at 1045 cm^{-1}. Thus, the IR spectra would make it apparent if the nitride was still present after reactions designed to remove chlorines were performed. The two approaches used for the removal of the chlorides were by reduction of the molybdenum and replacement of the chlorides by substitution with other ligands. In some cases both approaches were combined in one reaction.

The first set of reactions involved the ammonolysis of $MoNCl_3$ in the attempt to replace the chlorides with amido groups. The reactions were carried out by distilling ammonia onto the $MoNCl_3$ to give a red solution. The solution was then stirred for 2 - 3 hours at -45°C, during which the solution turned dark purple. The solution was then warmed to allow the ammonia to boil off and a black precipitate formed. The solid was then extensively washed with liquid ammonia to remove the NH_4Cl that was formed. The reaction has been formulated as follows:

$$MoNCl_3 + xsNH_{3(l)} \longrightarrow MoNCl_{4/3}(NH_2)_{5/3}\bullet 2NH_3 + 5/3\ NH_4Cl \quad (5)$$

The product of this reaction was insoluble in all organic solvents in which it did not react. Anal. Calculated for $MoNCl_{4/3}(NH_2)_{5/3}\bullet 2NH_3$: Mo, 44.0%; Cl, 21.69%, oxidation state, +6.0. Found: Mo, 43.7%; Cl, 21.54%; oxidation state, +6. The infrared spectrum of this compound was very simple

with few peaks. The most obvious change from $MoNCl_3$ was the presence of a broad band at 3100 cm^{-1} which can be ascribed to N-H stretching. There were two fairly sharp bands at 1600 and 1270 cm-1 which are the asymmetric and symmetric deformation modes, respectively, of NH_3 and NH_2 groups. The band which corresponds to ν (Mo≡N) has shifted to a lower frequency, from 1045 cm^{-1} to 1020 cm^{-1} and was slightly broadened. The remaining bands at 850 and 450 cm^{-1} were assigned as ρ (NH_3) and ν (M-N) modes. Below ~335 cm^{-1}, the spectrum tails off and did not show the expected bands from Mo-Cl vibrations; however, chlorine is obviously present from the chemical analysis.

The formulation of this species was close to the desired product since the species contains very little chlorine, a great deal of nitrogen and small quantities of other elements, besides the molybdenum, and the latter is in a high oxidation state. The determined stoichiometry indicates a mixture of compounds due to the fractional quantities of chlorine and amides. The insolubility of this compound in organic solvents indicates that it may be polymeric. The next process for conversion to the nitride would be removal of the hydrogen atoms, most likely as ammonia, as well as the remaining chlorides. This would undoubtedly require more rigorous conditions, since the final chloride remained bonded to the molybdenum throughout the previous steps.

Numerous attempts were made to drive off the remaining chlorine by using thermal methods. The heating of $MoNCl_{4/3}(NH_2)_{5/3} \bullet 2NH_3$ in a dynamic vacuum at 250°C for ≥ 8 hours gave a black product from which some ammonium chloride was sublimed. This product was amorphous to x-rays and showed only a few very weak bands in the IR spectrum. The IR frequencies were at 3135 cm^{-1} (ν NH), 1651 cm^{-1} (δ NH_2), 1020 cm^{-1} (ν Mo≡N), 974 cm^{-1} (NH_2), and a very sharp band at 315 cm^{-1} which was probably due to an Mo-Cl stretching vibration. Chlorine was still present in the product at slightly higher percentage than the $Mo(N_3)Cl$, but some ammonia was lost so this increase in percentage of chlorine with a loss of ammonium chloride can be explained. Heating the sample to 400°C in a vacuum did not crystallize the product but it did eliminate all bands in the IR spectrum. Anal. Found: Mo, 70.0%; Cl, 24.43%. This shows that even in the high temperature treatment, the chlorine was not completely removed even though a great deal of the nitrogen had been. When the reaction at 400°C was performed in flowing ammonia, chlorine was present at a much lower percentage. Anal. Found: Mo, 77.8%; Cl, 7.22%; Cl/Mo, 0.25. The product was still not crystalline and gave an IR spectrum that had very little transmittance and no peaks. The removal of the final chlorine atoms therefore requires a different approach, since ammonolysis did not appear to give the desired nitride. The next procedure involved the use of sodium

amide in an attempt to remove the chlorine atom and form the molecular precursor $MoN(NH_2)_3(NH_3)_2$.

The reactions of $MoNCl_3$ with sodium amide in liquid ammonia gave very similar results to those of the ammonolysis of $MoNCl_3$. The addition of $NaNH_2$ had to be performed after the dissolution of the $MoNCl_3$, because when the two were mixed together as solids, an energetic reaction took place accompanied by a flash and smoke. Upon mixing the reactants in ammonia, the solution turned from red to deep purple, and then a black precipitate formed as the mixture was warmed to remove the ammonia. The reaction has been formulated as follows:

$$MoNCl_3 + 8/3\ NaNH_2 \longrightarrow MoNCl_{1/3}(NH_2)_{8/3} + 8/3\ NaCl \qquad (6)$$

The reactant ratio used in the reaction was one $MoNCl_3$ to three sodium amides with a slight excess of the sodium amide to insure complete reaction; however, the formulation above was determined from the analysis of the products. The observed and calculated percentage compositions were in good agreement. Anal. Calculated for $MoCl_{1/3}N_{11/3}H_{16/3}$: Mo, 58.35%; Cl, 7.19%. Found: Mo, 57.9%; Cl, 7.26%. The oxidation state of Mo was found to be +6. The IR bands and their assignments were 3136 cm^{-1} ν (N-H), 1603 cm^{-1} δ (NH_2), 1024 cm^{-1} ν (Mo≡N), 810 cm^{-1} ρ (NH_2), and 455 cm^{-1} ν (MN).

While this appeared to be a better method for the removal of chlorine from these systems, a small portion of chlorine still remained in the formula unit. Using moderate temperatures and flowing gases to further remove chlorine from this compound gave products with identical characteristics to those derived from the $MoNCl_3$ ammonolysis product reported previously. Without using extreme conditions, it appeared that the removal of the remaining chlorine would not be readily observed by using the methods described here.

The next series of reactions involved $MoNCl_3$ with trimethylsilylazide and hexamethyldisilane (HMDS). The use of these reagents was based on the idea that TMSA would produce the azido compound $MoNCl_2(N_3)$, and the HMDS would then promote decomposition of the azide with removal of the chloride ligands. These ideas are summarized in the reactions:

$$MoNCl_3 + (CH_3)_3SiN_3 \longrightarrow MoNCl_2(N_3) + (CH_3)_3SiCl \qquad (7)$$

$$MoNCl_2(N_3) + Si_2(CH_3)_6 \longrightarrow MoN_2 + 2(CH_3)_3SiCl + N_2 \qquad (8)$$

The reaction of $MoNCl_3$ with trimethylsilylazide was performed in refluxing chlorobenzene. After two days a bright red solid was observed in the flask. The product was filtered and then dried. While the product was still moist from the solvent, there were no difficulties in handling it, but upon

drying it became extremely shock sensitive, exploding at the slightest provocation. It was assumed that the product was $MoN(N_3)Cl_2$ because of this behavior. Further experiments along this line were discontinued due to extreme hazard. Reactions of $MoNCl_3$ first with $(CH_3)_3SiN_3$ and then $Si_2(CH_3)_6$ were not attempted because of the formation of azido compounds during the same reactions with $WNCl_3$, which will be discussed later. The molybdenum azide compounds appear to be much more unstable than the tungsten compounds, although both are energetic materials.

The reaction of excess hexamethyldisilane with $MoNCl_3$ in refluxing dichloroethane gave a reduced species. The reaction began immediately upon mixing of the reactants, with the solution turning a dark reddish brown and a similarly colored precipitate falling out of solution. The product was filtered and the elemental analysis performed. Anal. Calculated for $MoNCl_2$: Mo, 53.0%; Cl, 39.20%. Found: Mo, 52.9%; Cl, 39.40%. The chlorine to molybdenum ratio was determined to be 2.02, which was in good agreement with that expected for $MoNCl_2$. The infrared spectra changed very little from $MoNCl_3$ with a sharp peak at 1045 cm^{-1} ν (Mo≡N) and peaks at 410, 376, and 320 cm^{-1} ν (Mo-Cl). The reaction was determined to be:

$$2\ MoNCl_3 + xs\ Si_2(CH_3)_6 \longrightarrow 2\ MoNCl_2 + 2\ (CH_3)_3SiCl \quad (9)$$

The hexamethyldisilane partially succeeded in removing the chlorine from the $MoNCl_3$ but it was not a strong enough reducing agent to give the chlorine free species.

The reactions attempted using molybdenum chlorides as the starting materials gave a variety of compounds, however none of them had the desired composition to serve as effective precursors for the preparation of nitrides at low temperatures. Further studies will need to be undertaken to find reducing agents and nitrogen compounds which will remove the remaining chlorines from the system. Next the research performed in the tungsten system will be discussed .

Tungsten Chemistry

The methods used to prepare the tungsten compounds were similar to those used for the molybdenum compounds. The only starting materials used in the tungsten case were those where the tungsten was already in the +6 oxidation state, namely WCl_6 and $WNCl_3$. The first part of this section will deal with reactions of the tungsten nitride chloride with hexamethyldisilane and trimethylsilyl azide for the removal of chlorine and the addition of nitrogen, respectively. The second part describes the more promising

reactions involving ammonolysis and the subsequent transformation of the products to novel compounds.

The reactions involving the use of $Si_2(CH_3)_6$ and $(CH_3)_3SiN_3$ were carried out in hydrocarbon solvents under inert atmospheres. In experiments which involved only the hexamethyldisilane, the observed reactions were:

$$WNCl_3 + 1/2\ Si_2(CH_3)_6 \longrightarrow WNCl_2 + (CH_3)_3SiCl \qquad (10)$$

$$WNCl_3 + xs\ Si_2(CH_3)_6 \longrightarrow WNCl_{3/2} + 3/2\ (CH_3)_3SiCl \qquad (11)$$

In both of the above reactions, the HMDS was added by syringe to a dichloroethane solution of $WNCl_3$. Reaction occurred immediately upon the addition of the HMDS giving a dark reddish brown solid. The chemical analysis of the product from the first reaction agreed well with the formulation in equation 10. Anal. Calculated for $WNCl_2$: W, 68.7%; Cl, 26.38%. Found: W, 68.2%; Cl, 26.5%. The chlorine to tungsten ratio for the product was found to be 2.01. In the second reaction, an excess of HMDS was used and the solution was refluxed to ensure complete reaction, the chlorine to tungsten ratio was found to be 1.50 and the formulation of the product was $WNCl_{3/2}$. Anal. Calculated for $WNCl_{3/2}$: W, 73.4%; Cl, 21.18%. Found: W, 74.0%; Cl 26.38%. The infrared spectra for both of these products were very simple and similar to $WNCl_3$, giving bands at 1070 cm^{-1} and a couple of

bands for metal-chlorine stretches below 350 cm^{-1}. In these cases, it appeared that the $Si_2(CH_3)_6$ was not a strong enough reducing agent to remove all of the chlorines and give the tungsten(III)nitride. It is conceivable that no reagent will be effective in forming the solid WN directly from a low temperature route in the absence of a sintering step.

When reactions were tried in which TMSA was used in combination with HMDS, the results were not wholly unexpected. The reason for not using the TMSA alone was because explosive azido compounds would be formed. It was hoped that the HMDS would remove chloride by reduction and induce the azido intermediate to decompose into the nitride and nitrogen. It has already been shown that the species $W(N_3)Cl_5$ and $W(N_3)_2Cl_4$ are explosive[17], so the reduction of the azides prior to isolation was an important consideration. The reactions were performed by addition of the $(CH_3)_3SiN_3$ to an orange DCE solution of $WNCl_3$, which resulted in a dark red solution, and then addition of $Si_2(CH_3)_6$, which gave a bright red solution. The mixture was then refluxed for three to six hours and during this time the solutions turned dark brown and gave a brown precipitate. The products were then extracted with the reaction solvent. If the HMDS was added first, the only products observed were those from the previous reactions, Eqns. 10 and 11, which did not involve azide. All of these products were pyrophoric and insoluble in all organic solvents with which they did not react. During

dissolution of samples to perform the analytical work, the effects of trimethylsilyl compounds, such as the expansion of blood vessels in the sinuses and eyes, were quite noticeable. For the material isolated from the reactions where both TMSA and HMDS were used, the following data were obtained. Anal. Found: W, 43.8%, Cl, 8.38%; Cl/W, 0.992. The infrared spectra gave a number of bands which were assigned as follows (all values given in cm^{-1}): 2125, 2087, and 1310 ν (N_3); 1649 (uncertain assignment); 1252 and 1150 ρ (CH_3); 918 and 845 ν (Si-C); 400 and 350 ν (W-Cl). The most obvious conclusions were that an azide group was still present and a silicon nitrogen bond appeared to have been formed. A possible formulation of the reaction was:

$$WNCl_3 + 2(CH_3)_3SiN_3 + (CH_3)_6Si_2 \longrightarrow WN(N_3)[N\{Si(CH_3)_3\}_2]Cl + (CH_3)_3SiCl + N_2 \quad (12)$$

Even though these reactions were attempted in higher boiling point solvents such as chlorobenzene, the azide compounds were not destroyed as shown by the IR spectrum. The species did not appear to be explosive upon shock testing, but such azides have a history of being sensitive. It was therefore decided to curtail experiments with these compounds, since we did not have the proper facilities to safely work with and characterize them.

The reaction of $WNCl_3$ with liquid ammonia was performed in the same manner as the ammonolysis of $MoNCl_3$. The ammonia was distilled onto the orange $WNCl_3$, forming a reddish orange solution. The condensation of the ammonia on the $WNCl_3$ was performed slowly, keeping the NH_3 frozen. If the process was carried out too quickly, the temperature of the mixture became too high and a violent reaction with explosive character ensued. The solution was stirred for about one hour at -45°C, during which it turned dark purple. The reaction mixture was then allowed to warm up slowly for the removal of the excess ammonia and a black precipitate came out of solution. Ammonia was then distilled onto the mixture a second time to ensure complete reaction. The products were then extracted with liquid ammonia to remove the NH_4Cl formed in the reaction. The reaction was determined to be:

$$WNCl_3 + 6\,NH_{3(l)} \longrightarrow WNCl(NH_2)_2(NH_3)_2 + 2NH_4Cl \qquad (13)$$

The product was insoluble in organic solvents as well as NH_3 and reacted with THF giving off a gaseous product, probably nitrogen or ammonia. The chemical analysis agreed well with the formula $WNCl(NH_2)_2(NH_3)_2$. Anal. Calculated: W, 61.43%; Cl, 11.84%; oxidation state, +6.0. Found: W, 61.4%; Cl, 11.37%; oxidation state, +6.0. The infrared spectrum showed the peaks expected for an amide with a broad peak at 3100

cm^{-1} ν (NH), medium peaks at 1593 and 1302 cm^{-1} δ (NH_2) or δ (NH_3). Further features included a medium band at 1020 cm^{-1} ν (W≡N), another at 845 cm^{-1} (uncertain assignment, possibly ρ(NH_3)), 460cm^{-1} ν (M-N) and 340 cm^{-1} ν (W-Cl). These bands agree with the formulation as it is written.

When $NaNH_2$ was used as a reactant in liquid ammonia at -45°C, the reaction appeared to take the course shown in Equation 14.

$$WNCl_3 + 2.5\ NaNH_2 \longrightarrow WNCl_{1/2}(NH_2)_{5/2}{\bullet}xNH_3 + 2.5\ NaCl \quad (14)$$

Conditions of this reaction were similar to those described by Eqn. 13, except that the product had to be washed many more times to ensure for the removal of NaCl and $NaNH_2$, due to the low solubility of $NaNH_2$. Anal. Found: W, 74.8%; Cl, 7.21%; oxidation state, +6.0; Cl/W, 0.5. These data would give a value of x in Eqn. 14 of about 0.25. The IR spectrum gave these frequencies: 3150, 1605, 1018, 847, 495,458 and 350 cm^{-1}, which can be assigned as in the previous case. The further processing of these compounds was then undertaken to prepare the nitrides, which will be discussed next.

The first attempt at formation of a nitride was the reaction of $WNCl(NH_2)_2(NH_3)_2$ in flowing ammonia at 250°C for approximately eight hours. Some ammonium chloride was observed at the cool end of the reaction tube. The IR showed peaks at 3100, 1736, 1599, 1288, 1020 cm^{-1}, and very

weak peaks at 400 and 340 cm^{-1}. This indicated that NH_2 groups were still present in the compound as well as chlorine. Anal. Found: W, 70.7%; Cl, 10.77%; Cl/W, 0.8. Longer reaction times did not appreciably change the chlorine content of the product. More rigorous conditions were obviously necessary for the complete removal of the chlorine, and the same reaction conducted at 380°C, again in flowing ammonia, proved to be the method for obtaining the chlorine free product. The reaction can be written as follows:

$$3WNCl(NH_2)_2(NH_3)_2 \longrightarrow 3W(NH)_2 + 3NH_4Cl + N_2 + 4NH_3 \quad (15)$$

The IR spectrum of this compound showed very poor transmittance, a large amount of background, and there were no observable peaks. This product was also amorphous by x-ray diffraction, so no structural data could be obtained in this manner. Anal. Calculated for $W(NH)_2$: W, 85.96%; oxidation state, +4.0. Found: W, 85.9%, oxidation state, +4.08. This compound was also insoluble in organic solvents and did not readily react with water. It appeared to be air-stable; the tungsten analysis did not change after exposure of the sample to air for a week. A thermogravimetric experiment, see Figure I.1, was run on a 9.00 mg sample of this product. It can be seen on the plot that there were two regions of weight loss during the experiment. Upon initial heating, there was a gradual loss of weight until

the temperature reached 500°C, whereupon the weight leveled off at 8.55 mg. Then, when the temperature reached about 580°C, there was a sharp drop in weight to 7.60 mg, where it remained until a slight weight gain was seen at 850°C. The latter was assumed to arise from a small amount of oxidation. The powder pattern of the final product of this thermolysis showed the presence of lines for tungsten metal and weak lines for WO_3. The weight loss of the compound, assuming tungsten is the final product, corresponds well with that expected from $W(NH)_2$. A cursory SEM-EDX analysis of $W(NH)_2$ showed that the only elements present with atomic number greater than four were tungsten and nitrogen. The solid state ^1H NMR spectrum was obtained to see if anything could be determined about the nature of the hydrogen atoms present. Figure I.2 shows the resolution enhanced spectrum with two very broad peaks having chemical shifts at 2.34 and 6.76 ppm. Since the shifts cover the area from 0.0 to 10.0 ppm, the only conclusion that could be inferred was that there was more than one kind of hydrogen present in the system.

The conditions for making the diimide appear to be very narrow. If the temperature was increased to much over 400°C, reduction occurs and there was formation of tungsten metal; if the temperature was below 380°C there is retention of chlorine. The use of nonreducing gases, such as nitrogen or

argon, could also allow the formation of tungsten metal at temperatures above 400°C and retention of chlorine at lower temperatures.

Reactions of $W(NH)_2$

The next step was to attempt to prepare a nitride or at least to obtain the diimide in crystalline form. In these experiments, the diimide was subjected to heating at varying temperatures under several different types of atmosphere. The conditions used included temperatures ranging from 300°C to 800°C and the gases used were ammonia, nitrogen, and argon. Heating in vacuum, both dynamic and static, was also examined. All of the reactions were carried out in sealed fused silica tubes on either loose powders or pressed pellets with rigorous exclusion of air.

In the annealing experiments, when reaction temperatures above 500°C were used, the products observed were gray powders which, based upon the x-ray powder pattern, proved to be tungsten metal. This result is not very surprising considering the thermodynamic studies by Lyutaya[13] and Lakhtin *et al.*[14] which show that at higher temperatures, the elements are more stable than the nitrides. It also showed that any species prepared in the present study would not be likely to be found as a product in high temperature syntheses. Decompositions performed in a vacuum, whether

static or dynamic, always gave tungsten metal as the product. When atmospheres of nonreactive gases, e.g., Ar or N_2, were used a weight loss occured, even at relatively low temperatures (~ 350°C). If the reaction proceeded long enough, tungsten metal was observed in the powder pattern. In these efforts to obtain crystalline $W(NH)_2$ by annealing, it appeared that the products were not stable enough at these temperatures to realize crystallization before dissociation occurred.

High temperature annealing reactions in ammonia gave similar results. At temperatures over 450°C in static pressures of ammonia ranging from one to eight atmospheres, disproportionation and/or reduction always occurred giving tungsten metal. Again, any compounds formed appear to be too unstable and decomposed under these conditions.

Results obtained from low temperature annealing in ammonia were much different, however. When a pressed pellet of $W(NH)_2$ was heated to 360°C in ~1.5 atmospheres of ammonia, a black crystalline material was obtained. Anal. Found: W, 80.5%; oxidation state, +5.2. The infrared spectrum gave very little transmittance but there were observable peaks at 1400, 970, a broad peak at ~800, 565, 420 and at 360 cm^{-1}. The lower frequency bands (< 600 cm^{-1}) could be due to M-N stretches while the higher ones (> 900 cm^{-1}) may arise from N-H vibrations.

Because air and oxygen were rigorously excluded in these experiments, the only elements present in the product should be tungsten, nitrogen and hydrogen. Given the oxidation state and percentage of tungsten, it appears that the compound formed was a triimmide. The compound did give an x-ray powder pattern, which can be seen in Figure I.3 and for which the lines are listed in Table I.1. This pattern matched the pattern for a hexagonal tungsten bronze of rubidium, $Rb_{0.27}WO_3$[23]. The cell parameters calculated from these x-ray data for this compound using a hexagonal setting are a = 7.394(2) Å and c = 7.521(4) Å. Also given in Table I.1 is the powder pattern calculated for the compound $(NH_4)_{0.33}W(NH)_3$ using the parameters from the rubidium tungsten bronze, which crystallizes in the $P6_3/mcm$ space group. A comparison of the calculated pattern to the experimental values shows very good agreement. At this point, a Rietveld refinement of the x-ray powder data of this imide bronze was undertaken and will be described later.

Experiments using longer annealing times gave similar results. Upon heating a pressed pellet of tungsten diimide for seven days at 355°C in ~1.5 atm. of NH_3 , a black compound was observed which gave the same powder pattern as that of the product in the three day reaction. The tungsten analysis in this case gave a slightly lower percentage at 74.2(1)%. For the theoretical compound $(NH_4)_xW(NH)_3$ with x=1, the tungsten analysis would show 74.48%. In the three day case the tungsten analysis was 75.2(1)%,

which would correspond to x = 0.87. When the reaction was run for 14 days on a loose powder, the tungsten analysis showed 74.4(1)%, which is virtually the same as the seven day case. The problem encountered here was that in the hexagonal bronze structure, the largest value that x can have is 0.33. This would tend to indicate that the species formed was not pure, with some other phase being present, which could explain the background undulation in the x-ray powder data, as discussed earlier. Longer reaction times did not significantly change the properties of the compound. The loose powder reaction products did not give any lines in the powder patterns, regardless of reaction time, so perhaps the pressed pellet is necessary in order for crystallization of the compound to occur. Four experiments were performed where the pressure was varied from ~0.75 to 10 atm and this did not affect the composition of the products so long as enough ammonia was present to complete the reaction. The IR spectra of the products annealed for longer than seven days were similar to that of the product of the three day reaction; however a broad peak at about 3000 cm^{-1} did appear, probably due to NH_4^+ being incorporated into the compound.

The TGA plots of the imide bronze compounds in flowing argon were similar to the tungsten diimide shown previously. As shown in Figures I.4 and I.5, the material underwent a gradual decrease in weight to a steady state at about 500°C and then a sharp weight loss at ~700°C. The main

difference was that the product of the runs was not tungsten metal, as was the case with the tungsten diimide. The weight loss was not great enough and the x-ray powder pattern showed no tungsten metal in the products. The powder pattern showed some lines of WO_3 plus others, but with the presence of oxygen in the system, it was difficult to make any conclusions about the product. The TGA plots of experiments run in air are shown in Figures I.6 and I.7. In all cases there was a weight loss until about 350°C and then steady state behavior was achieved. This would be consistent with the simultaneous removal of nitrogen and hydrogen (possibly as ammonia) and oxidation to WO_3. The mass of the product (WO_3) is also consistent with that expected from the tungsten analysis observed on the bulk materials.

A Rietveld refinement of the x-ray powder pattern of the tungsten imide bronze which had been annealed for three days was attempted using the parameters from $Rb_{0.27}WO_3$. The program used for the refinement was written by Wiles *et al.*[24] at the Georgia Institute of Technology and modified by Yingzhong Su in Professor Jacobson's group at Iowa State University. A slight problem was encountered in performing the refinement because of the background in the data. As can be seen in Figure I.3, the background of the x-ray powder pattern has a distinct dip at low 2θ angles and two broad peaks at approximately 26° and 37° in 2θ. These features could have a number of causes, such as a poorly crystalline second phase or perhaps some problem

with the way the data were collected (e.g., the sample holder was a glass slide). The poorly crystalline second phase could in actuality be the tungsten imide bronze since the two broad peaks correspond to two of the more intense peaks in the powder pattern. When a refinement was attempted on the untreated data, the refinement of the background did not match the experimental data very well and left a large Bragg R factor (~50%), even though the pattern R-factor and the weighted pattern R-factor were fairly small (~ 12% and 13%, respectively). It was then decided to strip the background in an attempt to compensate for the discrepancy.

In starting the refinement, the lattice parameters used were 7.394 Å and 7.521 Å for the a and c axes, respectively. The positional parameters used were 0.48, 0, 1/4 for the tungsten and 1/2, 0, 0 and 0.42, 0.22, 1/4 for the two imide nitrogen atoms. Initially, a nitrogen atom was placed in the position of the ternary cation for the M_xWO_3 bronze structure (at 0,0,0). However, during the refinement it was found that the multiplier, if varied, would go to zero leaving no atom in the position. The refinement involved 2703 data points, 60 reflections in the 2θ region from 10 to 64.04°, and the refinement of 21 parameters. Those parameters included 2 background parameters, a scale factor, a mixing parameter for the peak profile function (a pseudo-Voigt relationship), lattice constants, and positional and thermal parameters. The thermal parameters of the nitrogen atoms were only refined isotropically

since they always became nonpositive definite when anisotropic refinements were attempted. Table I.2 lists the refinement parameters and residual factors while Tables I.3 and I.4 give the positional and thermal parameters. Figure I.8 shows the 2θ profile of the Rietveld refinement. A close examination of the Figure I.8 shows that there was some broadening at the base of the peaks which could be caused by a problem with the data (e.g., the background) or the choice of the peak profiling function, which was not adequate for the conditions of data collection.

The structure of the tungsten imide bronze was nearly the same in all respects as that of the rubidium tungsten bronze, the only difference being the shifting of the N2 atoms toward the origin. This shifting of the atoms could be explained by the presence of hydrogen atoms bonded to the nitrogen atoms. For this to be the case, one could assume that the hydrogen atoms were occupying positions between a triangle of nitrogen atoms, see Figure I.9. Figure I.9 shows one layer of atoms in the unit cell with the N1 atoms omitted for clarity. Figure I.10 shows the tungsten atom positions (at z = 1/4 and 3/4) in the unit cell. It can be seen (Figure I.9) that the tungsten atoms reside in the middle of a rectangle of N2 atoms, and attain a coordination number of 6 with the N1 atoms (at 1/2, 0, 0) above and below the tungsten. The tungsten atom thus achieved a distorted octahedral coordination. There were three W-N distances in the WN_6 octahedra. Both W-N1 distances are

1.887 Å, and two W-N2 distances at 1.828(5) Å and 2.401(5) Å. Again, this long distance could be due to the presence of hydrogen atoms. The W-W distances are 3.713(1) Å in the ab plane and 3.775(1) Å along the c-axis. These values were comparable to those found in the hexagonal oxide bronzes. The site at 0, 0, 0 (which is occupied by the ternary cation in the oxide bronzes) appeared to be available for occupation by some species, so if the product can by made with tungsten in a more reduced state, any of a number of cations could be substituted in the compound.

There are a number of unsolved problems in the Rietveld refinement which will require further work. The broadening of the peaks at the base and the background of the x-ray powder pattern has to be taken into account as well as the inability to refine the thermal parameters of the nitrogen atoms anisotropically. The solution to all of these problems is probably to improve the quality of the x-ray data and therefore, the sample. A better sample, i.e., more crystalline and/or purer, needs to be prepared in order to clear up any ambiguities in this work. Perhaps a neutron diffraction study could be undertaken to determine the exact position of the hydrogen atoms.

SUMMARY

Several types of reactions were performed in order to prepare nitride precursors and nitride materials of tungsten and molybdenum using low temperature techniques. Using the chlorides as the starting materials, the compounds obtained showed varying amounts of residual chlorine bonded to the metal atoms. In the cases involving molybdenum, no materials were prepared which were chlorine free, even those obtained from reactions at moderately high temperatures. In the tungsten case, several compounds were made in which the chlorine to tungsten ratio was one or less. One of the compounds, $WNCl(NH_2)_2(NH_3)_2$, was treated in a stream of ammonia and gave the new chlorine free compound $W(NH)_2$. The further reaction of this compound in ammonia at 355°C produced a tungsten imide bronze similar to the hexagonal tungsten bronze M_xWO_3 ($x \leq 0.3$).

From this work, it has appeared that the removal of the remaining chlorine from the metal nitride chloride compounds would require more vigorous conditions or more reactive starting materials. The final metal to chlorine bond was too strong to allow the removal of the chlorine by the methods attempted to this point. The use of starting materials (nitrogen containing ligands) with more labile species, such as organic or organosilicon functional groups, may help facilitate the removal of the final chlorine. The

problem with this approach, as stated earlier, would be the introduction of another element, in addition to the metal and nitrogen, which could give unwanted products such as silicides and carbides. The use of different tungsten and molybdenum compounds as the metal source could also have some advantages. The fluorides may be good candidates because the strength of the fluorine silicon bond would help drive the replacement of fluoride to completion in a reaction with $((CH_3)_3Si)_3N$, for example. The difficulty in handling fluorine compounds would create a whole new set of problems in synthesis. Use of a stronger reducing agent could also help in removing the final chlorines from the chloride starting materials, but the reducing agent should not be so strong at to completely reduce the metal. When azide intermediates are used, photolysis reactions may assist in the splitting off of the nitrogen and the remaining chlorines to give the low temperature nitrides. Finally, the study of the tungsten imide bronzes should be expanded to obtain single crystals as well as to study the effect of different cations on the structure of the bronzes.

REFERENCES

1 a)Mazdiyasni,K.S.; Cer. Int. 1982, 8, 42
b)Roy,R.; Science 1987, 238, 1664

2 a)Rideal,S.; J. Chem. Soc. 1889, 55, 41
b)Smithells,C.J.; Rooksby,H.P.; J. Chem. Soc. 1928, 94, 1882
c)Mittasch,von A.; Frankenberger,W.; Z. Elektrochem. 1929, 35, 920
d)Boreskov,G.K.; Kolchanova,V.M.; Rachkovskii,E.E.; Filimonova,S.N. Khasin,A.V.; Kinet. Katal. 1975, 16, 1218
e)Kawai,T.; Kunimori,K.; Kondow,T.; Onishi,T.; Tamaru,K.; Phys. Rev. Lett. 1974, 33, 533
f)Aika,K.; Ohata,T.; Ozaki,A.; J. Catal. 1970, 19, 140
g)Yatsimirskii,V.K.; Markova,A.P.; Samsonov,G.V.; Tovbin,M.V.; Lyutaya,M.D.; Katal. Katal. 1971, 7, 771
h)Neugebauer,Von J.; Hegedus,A.J.; Millner,T.; Z. Anorg .Allg. Chem. 1959, 302, 50

3 Langmuir,I.; J. Am. Chem. Soc. 1914, 36, 931

4 Iwana,S.; Hayakawa,K.; Arizumi,T.; J. Cryst. Growth 1984, 66, 189

5 Pinsker,Z.G.; Khitrova,V.I.; Soviet Phys. Crystallogr. 1962, 6, 712 and references therein.

6 Gunther,F.; Schneider,H.G.; Soviet Phys. Crystallogr. 1967, 11, 585

7 a)Ihara,H.; Hirabayashi,M.; Senzaki,K.; Kimura,Y.; Kezuka,H.; Phys. Condens.Matter 1985, 32, 1816
b)Ettmayer,P.; Monatsh. Chem. 1970, 101, 127
c)Dawson,P.T.; Stazyk,S.A.J.; J. Vac. Sci. Technol. 1982, 20, 966

8 a)Yu,K.M.; Jaklevic,J.M.; Haller,E.E.; Cheung,S.K., Kwok,S.P.; J. Appl. Phys 1988, 64, 1284
b)Allen,D.A.; Herniman,J.; Gilbert,M.J.; O'Sullivan,P.J.; Grimshaw,M.P.; J. Phys. Colloq. 1988, C4, 427

9 a)Nagata,S.; Shoji,F.; Jap. J. Appl. Phys. 1971, 10, 11
b)Shoji,F.; Nagata,S.; Jap. J. Appl. Phys. 1974, 13, 1072

10 a)J. Vac. Sci. Technol. 1988, 6, 1717
b)Gicquel,A.; Bergongnan,M.P.; Amouroux,S.; Proc. Electrochem. Soc. 1983, 83, 169

11 Caillet,M.; Lagarde,Y.; Besson,J.; Rev. Chim. Miner. 1971, 8, 605

12 Schonberg,N.; Acta Chem. Scand. 1954, 8, 204

13 Lyutaya,M.D.; Soviet Powder Metall. Metal Cer. 1979, 190

14 Lakhtin,Yu.M.; Kogan,Ya.D.; Borovskaya,T.M.; Solodkin,G.A.; Russ. Metall. 1979(4), 158

15 Boyer,L.L.; Krakaur,H.; Klein,B.M.; Pickett,W.E.; Wang,C.S.; Physica B+C 1985, 135, 252

16 a)Watanabi,R.; Yazaki,I.; Igarashi,Y.; Toyota,N., Noto,K.; J. Mater. Sci. Lett. 1986, 5, 255
b)Papconstantopoulos,D.A.; Pickett,W.E.; Phys. Rev. B. Condens. Matter 1985, 31, 7083
c)Papconstantopoulos,D.A.; Pickett,W.E.; Klein,B.M.; Boyer,L.L; Phys. Rev. B. Condens. Matter 1985, 31, 572
d)Ihara,H.; Hirabayashi,M.; Senzaki,K.; Kimura,Y.; Kezuka,H.; Phys. Condens.Matter
e)Linker,G.; Smithey,R.; Meyer,O.; J. Phys. F 1984, 14, L115

17 Dehnicke,K.; Strahle,J.; Z. Anorg. Allg. Chem. 1965, 339, 171

18 Holste,G.; Schafer,H.; J. Less-Comm. Met. 1970, 20, 508

19 Elwell,W.T.; "Analytical Chemistry of Tungsten and Molybdenum" Pergamon Press Inc.,New York, 1971, 324

20 Diehl,H.; Smith,G.F.; "Quantitative Analysis",John Wiley & Son Inc. New York, 1952, 270

21 Banks,C.V.; O'Laughlin,J.W.; Anal. Chem. 1956, 28, 1338

22 Schweda,E.; Strahle,J.; Z. Naturforsch. 1981, 36b, 662

23 Magneli,A.; Acta. Chem. Scand. 1953, 7, 315

24 Wiles,D.B.; Sakthivel,A.; Young,R.A.; School of Physics, Georgia Institute of Technology, Atlanta, GA, 1988.

Table I.1 X-ray powder diffraction data for tungsten imide bronze

Experimental		Calculated[a]		
d-spacing	intensity[b]	hkl	d-spacing	intensity
6.398	s	100	6.403	45
3.752	s	002	3.753	60
3.696	m	110	3.697	26
3.336	w	111	3.318	18
3.240	w	102	3.243	15
3.204	vs	200	3.202	100
2.637	w	112	2.636	18
2.440	vs	202	2.438	65
2.305	vw	211	2.304	6
2.135	vw	300	2.134	7
1.880	vw	004	1.880	12
1.849	w-m	220	1.848	25
1.804	vw	104	1.804	7
1.777	vw	310	1.776	8
1.729	w	311	1.728	14
1.660	w-m	222	1.659	27
1.622	m-b	204	1.621	30
1.602	w-b	400	1.600	12
1.473	w-m	402	1.473	15
1.450	vw	313	1.449	9
1.319	m-w	224	1.318	19
1.218	vw-b	404	1.219	13
1.209	vw	420	1.210	10

[a]Calculated from the hexagonal bronze structure with the lattice parameters a = 7.394(2) Å, b = 7.394(2) Å, c = 7.521(4) Å.

[b]vs = very strong, s = strong, m = medium, w = weak, b = broad.

Table I.2 Crystallographic data for $W(NH)_3$

Crystal System: Hexagonal Space Group: $P6_3/mcm$ (no. 193)

Lattice Parameters:

a= 7.4015(8) Å c= 7.5186(4) Å

V= 356.70(8)Å Z = 6

Pattern Range (2θ),deg; steps:10 - 64.04, 2702

Step scan increments(2θ),deg: 0.02

Step scan count time,s: 5.4

No.of contributing reflections: 61

Zero Point Error (2θ),deg: 0.0168

No. of structural parameters: 21

No. of profile parameters: 2

$R_p(\%)^a$: 8.02

$R_{wp}(\%)^b$: 10.41

$R_e(\%)^c$: 2.31

$R_b(\%)^d$: 15.70

$^aR_p = \Sigma | Y_o - Y_c | / \Sigma | Y_o |$.

$^bR_{wp} = (\Sigma\omega(Y_o - Y_c)^2 / \Sigma\omega Y_o^2)^{1/2}$.

$^cR_e = ((N-P)/\Sigma\omega Y_o^2)^{1/2}$.

$^dR_b = \Sigma | I - I_o | / \Sigma I$.

Table I.3 Positional parameters for $W(NH)_3$

atom	sym. position	x	y	z	Occupation	U(ave) A^3
W	g (mm)	0.4768(4)	0.0	1/4	1	39.0
N1	f (2/m)	1/2	0.0	0.0	1	31.7(5)
N2	j (m)	0.3403(7)	0.1486(6)	1/4	1	39.0(5)

Table I.4 Anisotropic thermal parameters[a] for tungsten in $W(NH)_3$

Atom	U_{11}	U_{22}	U_{33}	U_{12}	U_{13}	U_{23}
W	50.3(1)	34.9(0)	30.7(1)	34.9(1)	0.0	0.0

[a] The general thermal parameter expression used was:
$\exp[-2\pi^2(U_{11}h^2a^{*2} + U_{22}kb^{*2} + ... + 2U_{23}klb^*c^*\cos\alpha^*)]$.

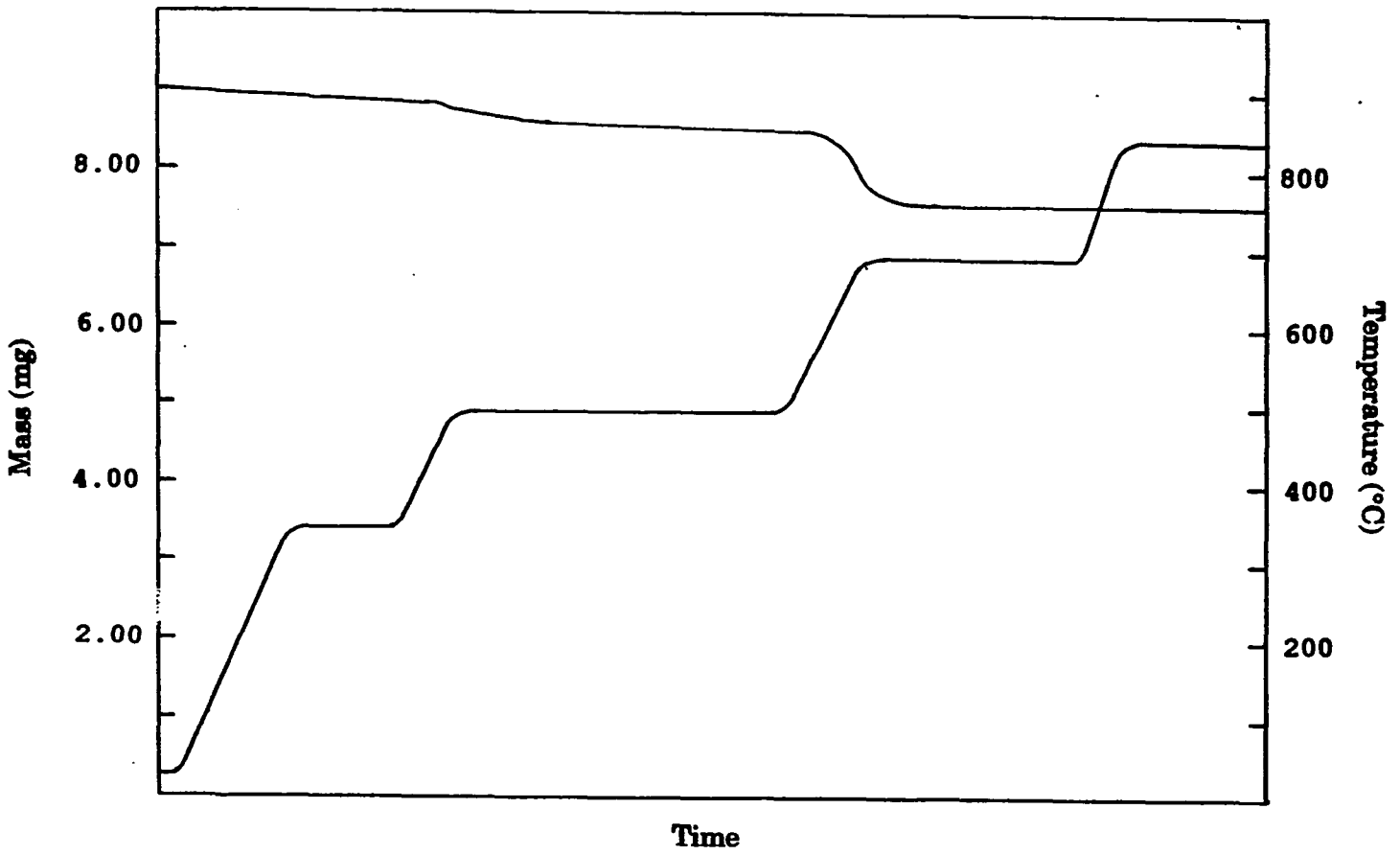

Figure I.1 The mass loss and temperature curves for the thermogravimetric analysis of $W(NH)_2$. The total time of the experiment was 174 minutes

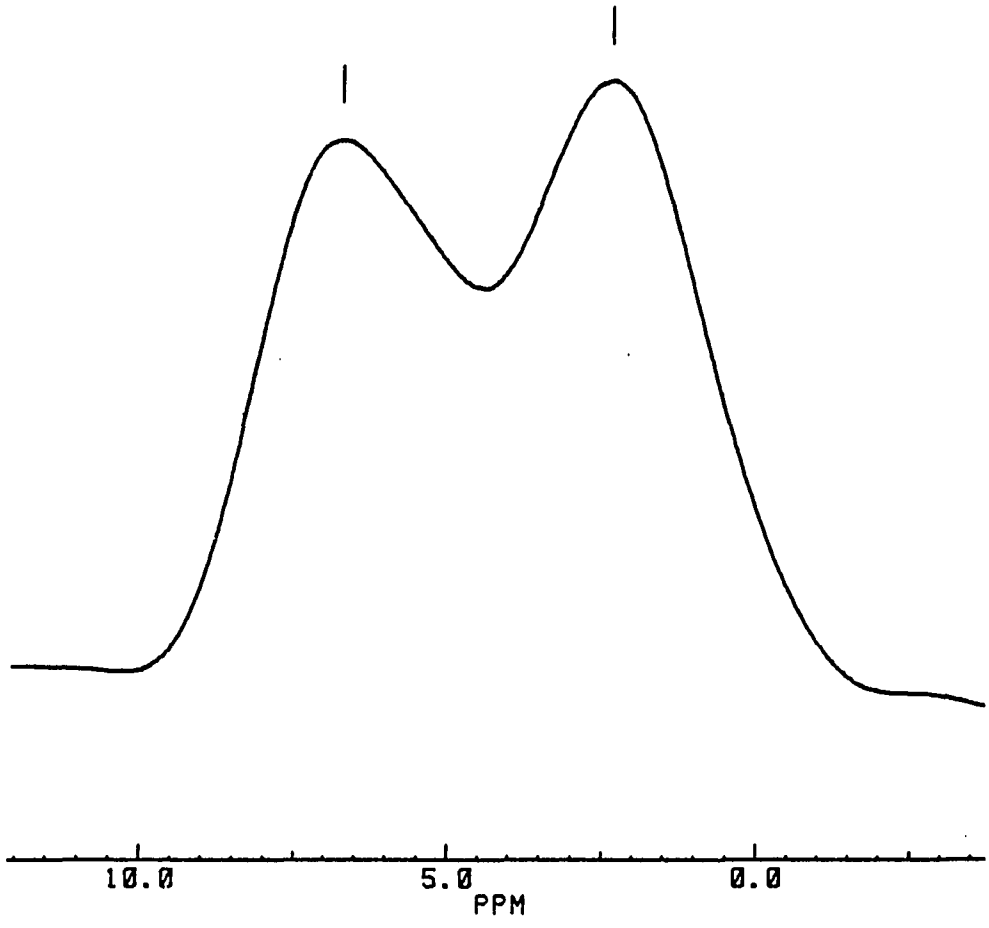

Figure I.2 The resolution enhanced solid state ^{1}H NMR of $W(NH)_2$ at 300 MHz. The pulse time was 1.5 μsec with a rotation frequency of 3924 rpm

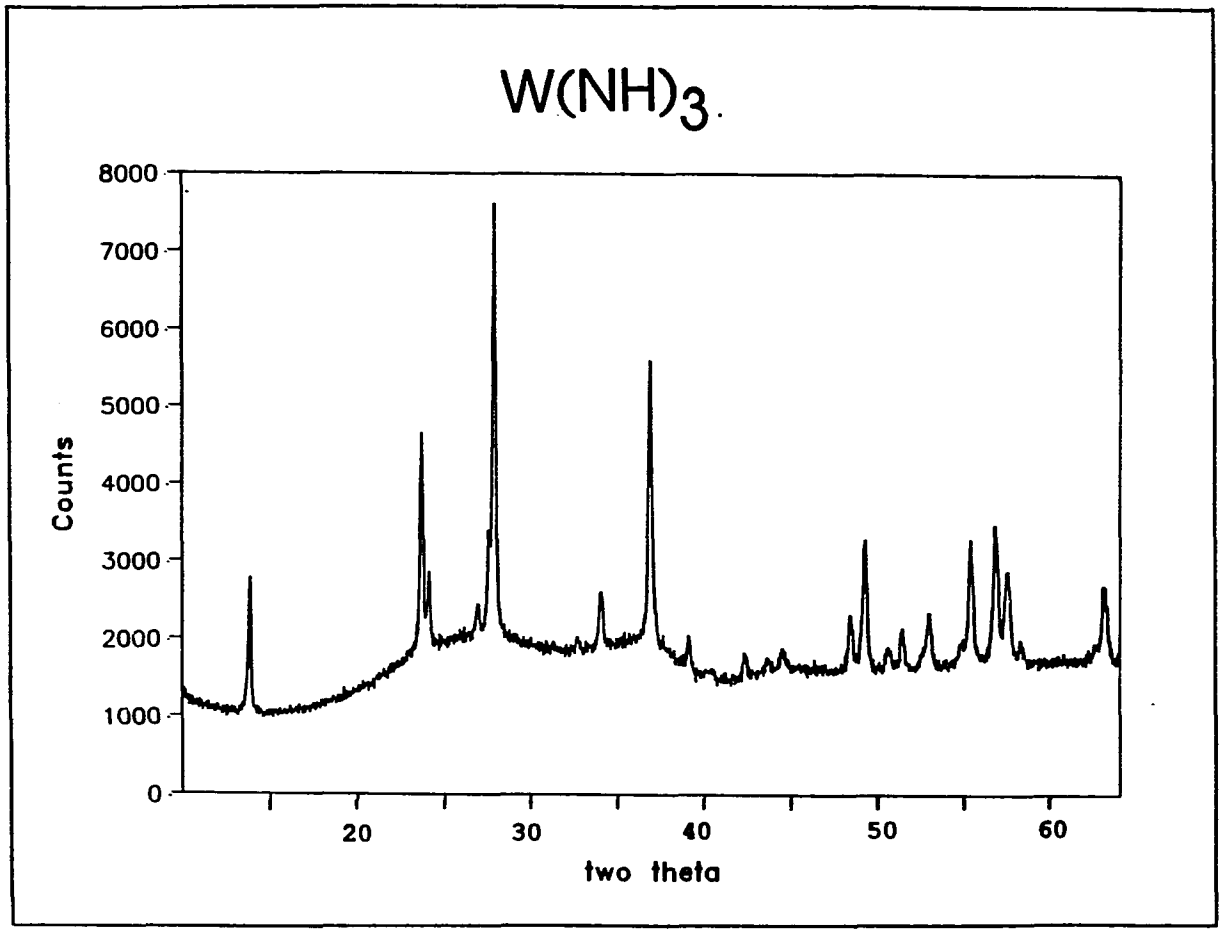

Figure I.3 **The x-ray powder pattern for the tungsten imide bronze**

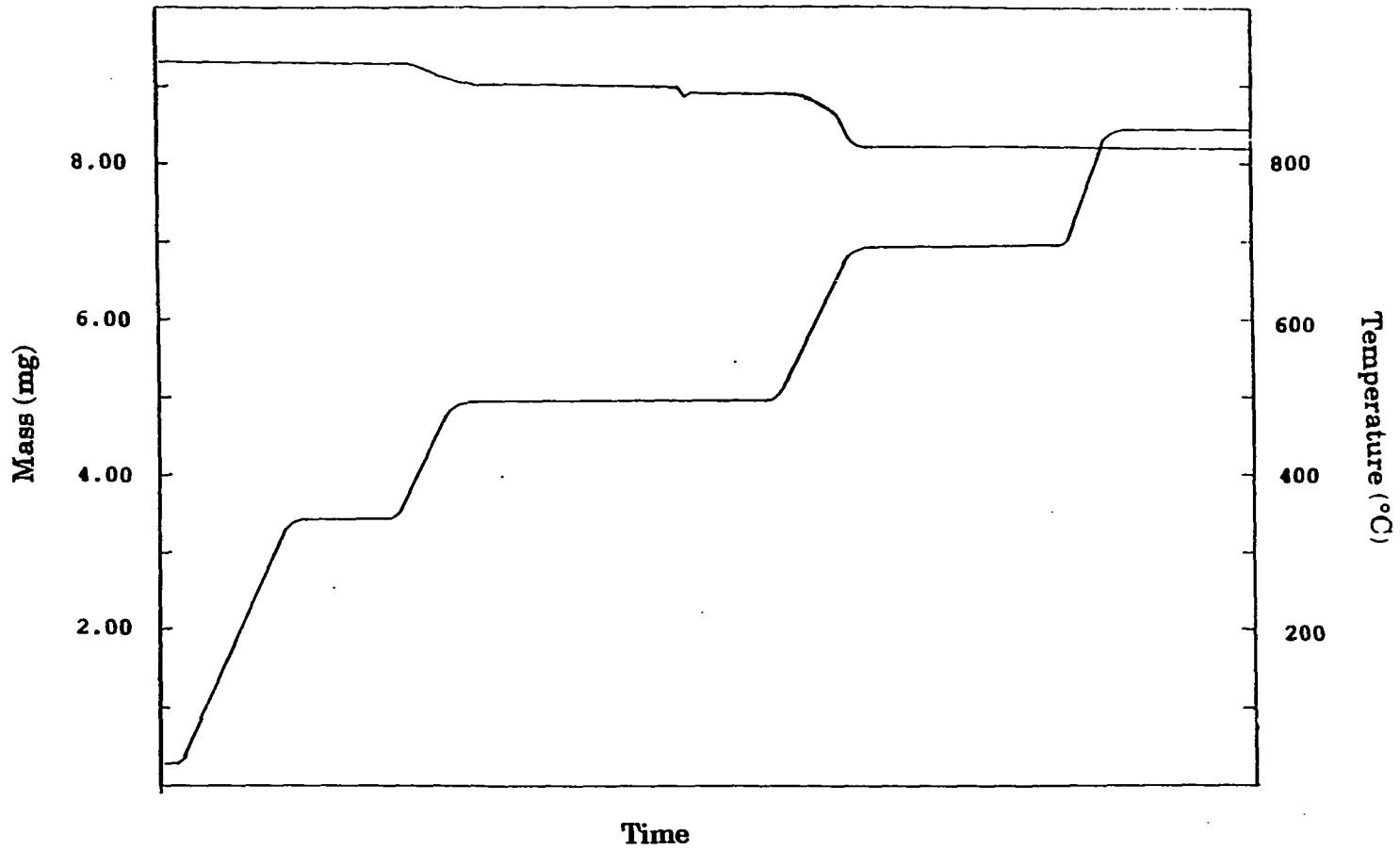

Figure I.4 The thermogravimetric plot, in argon, of the tungsten imide bronze formed in a three day reaction. The total time of the experiment was 174 minutes

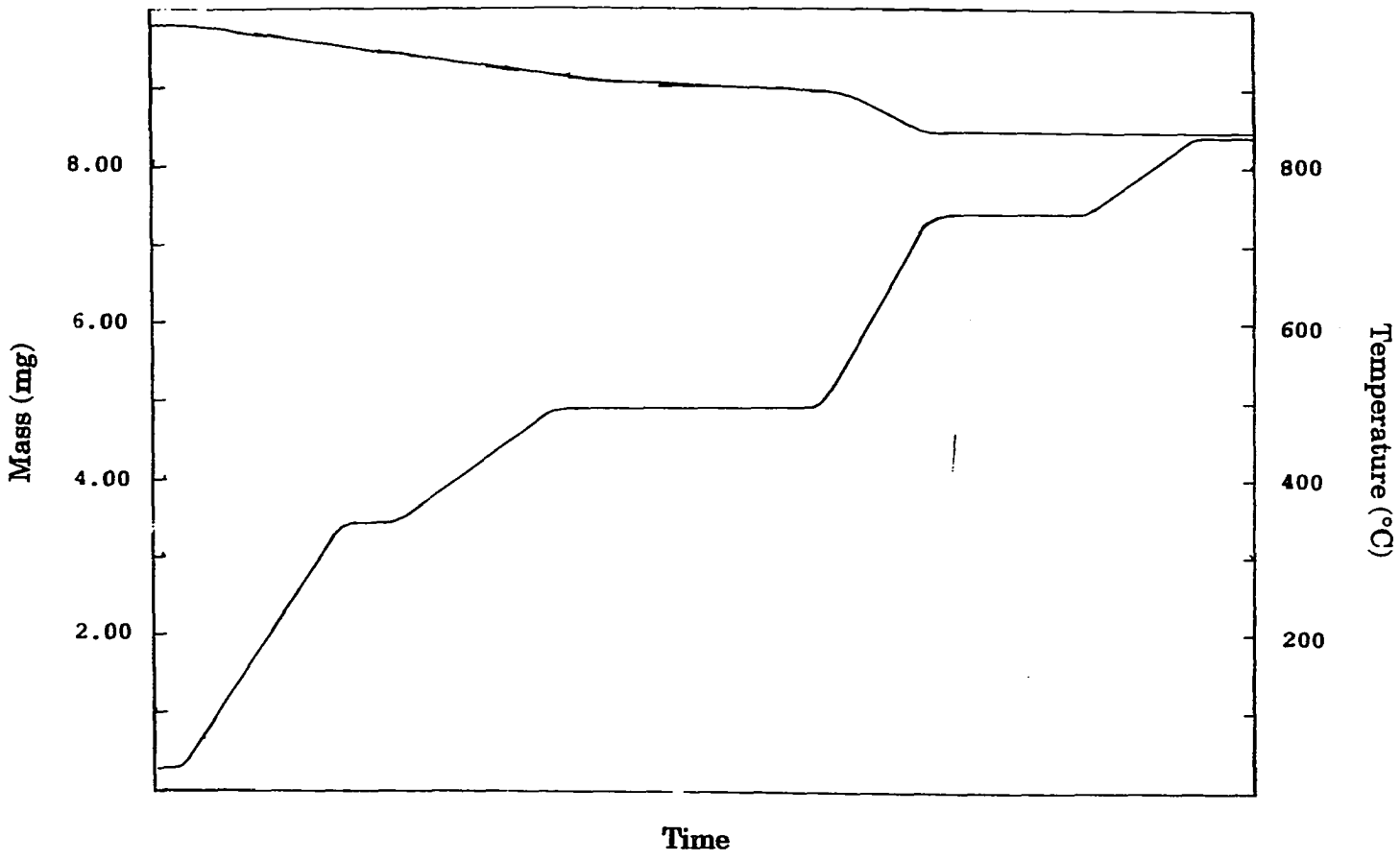

Figure I.5 The thermogravimetric plot, in argon, of the tungsten imide bronze formed in a seven-day reaction. The total time of the experiment was 174 minutes

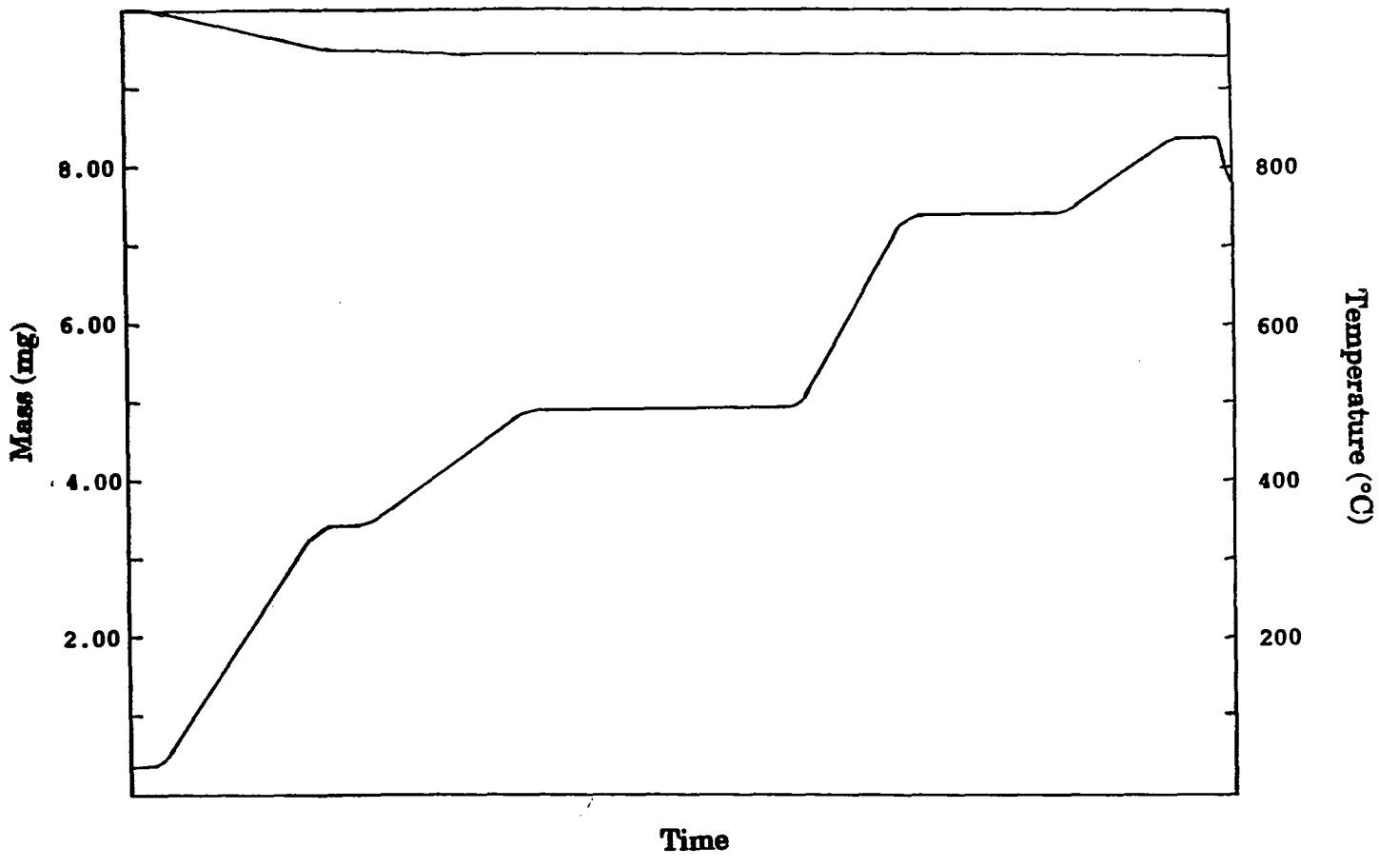

Figure I.6 The thermogravimetric plot, in air, of the tungsten imide bronze formed in a three day reaction. The total time of the experiment was 174 minutes

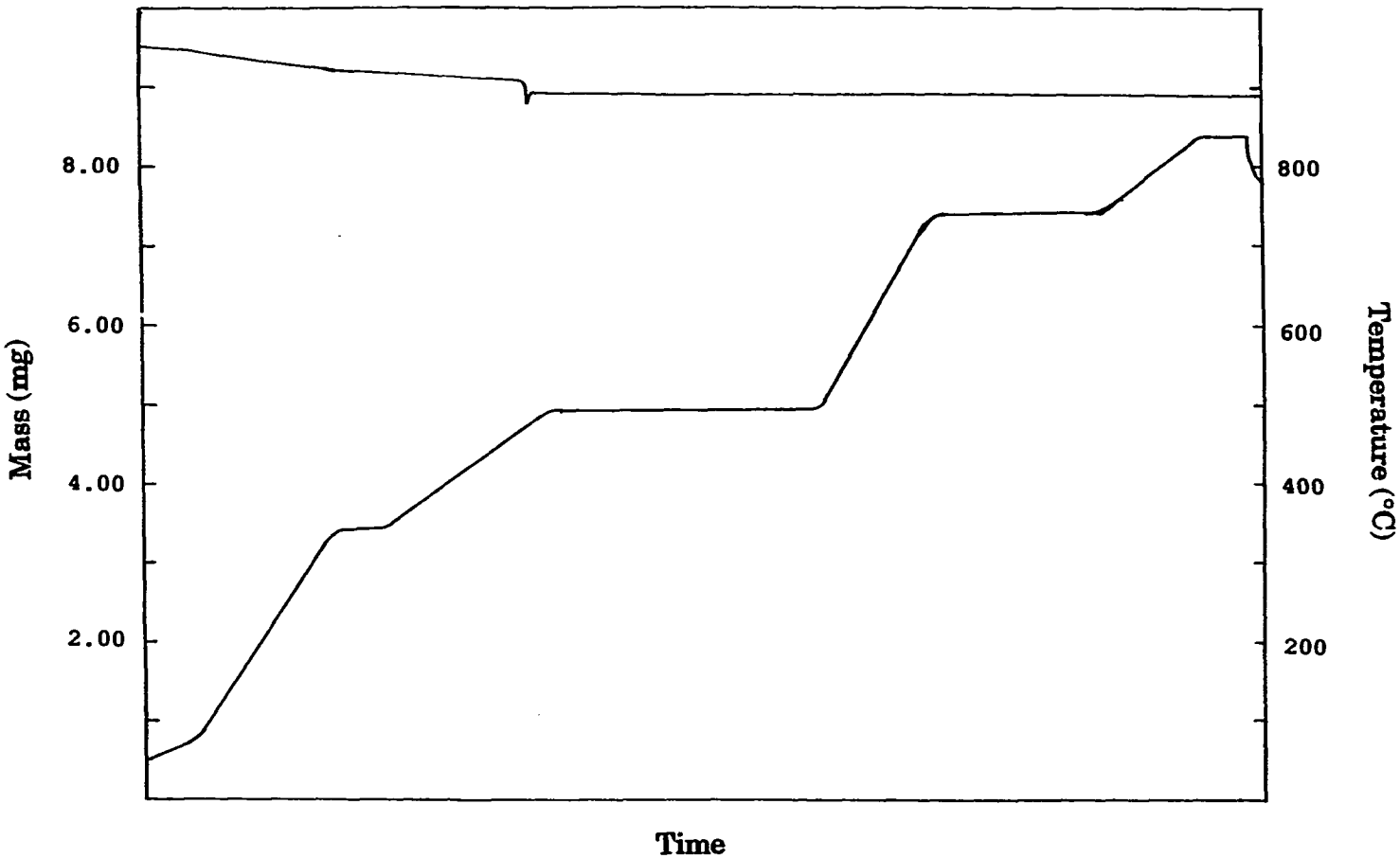

Figure I.7 The thermogravimetric plot, in air, of the tungsten imide bronze formed in a seven day reaction. The total time of the experiment was 174 minutes

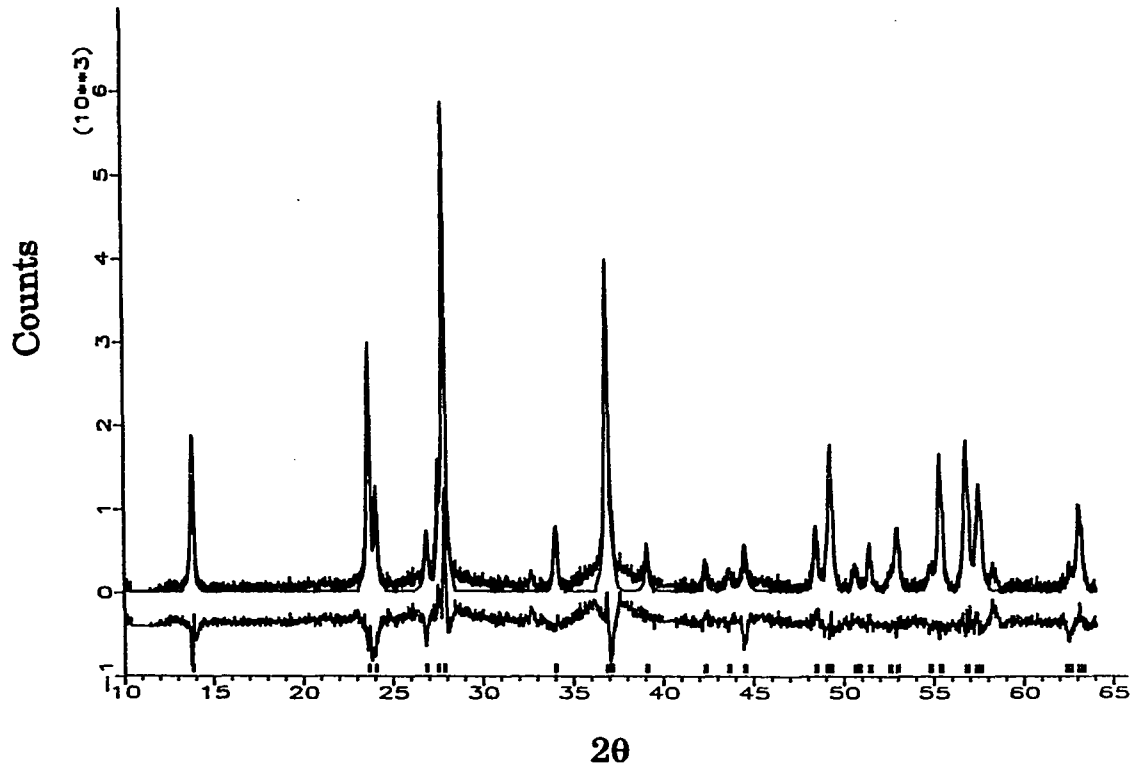

Figure I.8 The profile refinement of the 2θ data of $W(NH)_3$, ranging from 10 to 64.04°. The solid line indicates the calculated data and the difference curve appears at the bottom

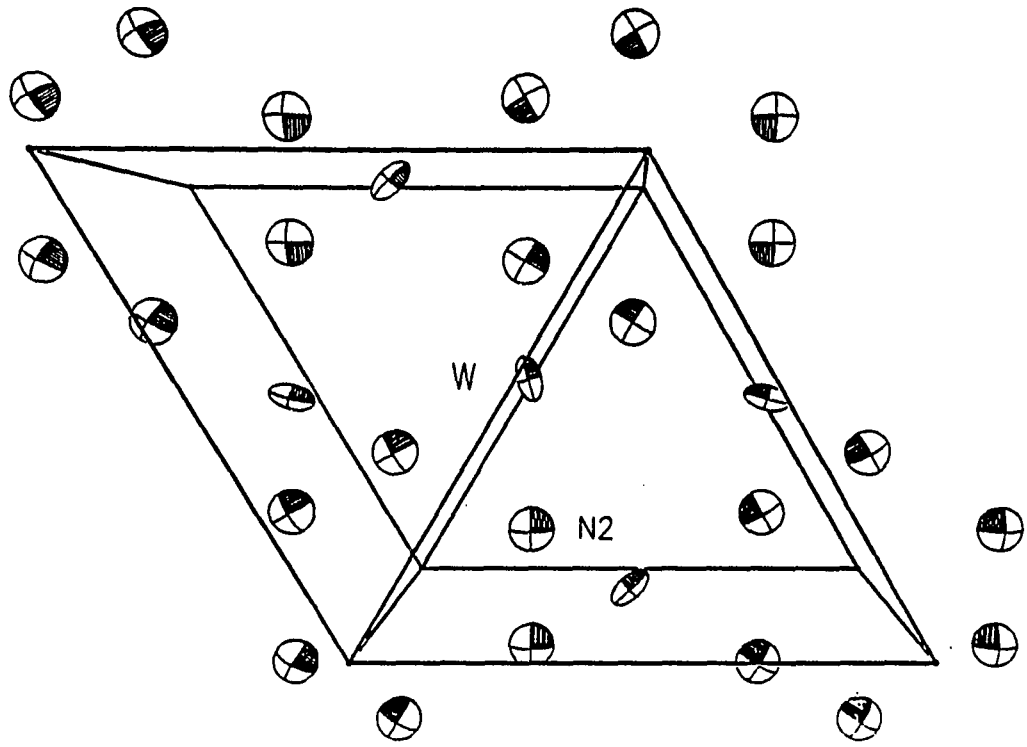

Figure I.9 An ORTEP drawing of one layer from the $W(NH)_3$ imide bronze. The N1 atoms, above and below each tungsten atom, have been removed for clarity. All atoms are represented by their 50% thermal ellipsoids

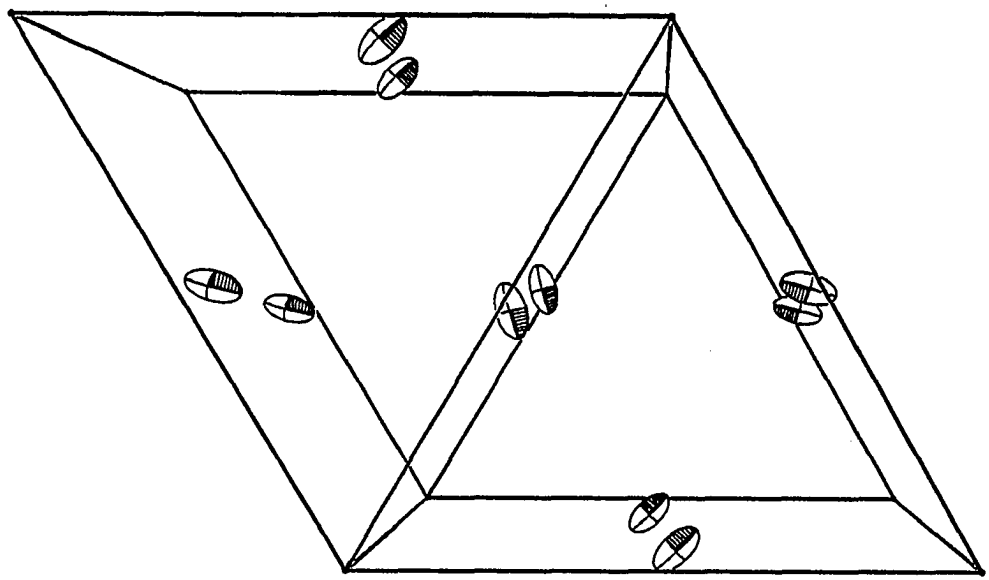

Figure I.10 An ORTEP drawing of the tungsten atoms in a unit cell of the $W(NH)_3$ imide bronze. The atoms are represented by their 50% thermal ellipsoids

Section II

PREPARATION AND STUDY OF SOME ANALOGUES OF $NdMo_8O_{14}$: COMPOUNDS WITH DISCRETE BICAPPED MOLYBDENUM OCTAHEDRAL CLUSTERS

INTRODUCTION

Reduced ternary molybdenum oxides have been studied extensively since the discovery of the compound $NaMo_4O_6$[1] in this laboratory. A large number of reduced compounds have been synthesized which contain various kinds of condensed metal clusters, from the infinite chains of edge-shared molybdenum octahedra in $NaMo_4O_6$ (a pseudo-one-dimensional compound) and $LiMo_8O_{10}$[2] (an interpenetrating network containing pseudo-one-dimensional orthogonal chains), to compounds containing metal-metal bonded rhomboidal clusters, as in $Ba_{1.14}Mo_8O_{16}$[3] (containing discrete Mo_4 units) and Na_xMoO_2[4] (containing one dimensional ribbons of fused Mo_4 units).

While discrete octahedral cluster units are well known in the Chevrel phase compounds and discrete rhomboidal clusters are seen in some reduced molybdenum oxides[3], discrete cluster units in the oxide system were rare until Simon and co-workers prepared the compound $In_{11}Mo_{40}O_{62}$[5] which contains discrete units of five and six edge-shared octahedra. Gougeon and McCarley, working in this laboratory, were able to prepare a discrete bicapped octahedral molybdenum cluster in a compound containing a rare earth element as the ternary cation[6]. The compound prepared was $NdMo_8O_{14}$. Recently, two other compounds with discrete molybdenum

clusters have been prepared, *viz.* $BaMo_6O_{10}$[7] and $La_2Mo_{10}O_{16}$[8], compounds containing a discrete octahedral cluster unit and an edge shared molybdenum bioctahedral unit, respectively.

The study of various analogues of $NdMo_8O_{14}$ was undertaken in an attempt to understand some of the features of this structure. The synthesis and physical measurements of a number of rare earth analogues to $NdMo_8O_{14}$ will be described in this section.

MATERIALS AND METHODS

The rare earth oxides (Ames Laboratory) were fired at 850°C overnight to remove the volatile constituents and then stored in a desiccator over $CaSO_4$. Molybdenum dioxide (Alfa Products, 99%) and molybdenum powder (Aldrich Chemical, 99.99%) were heated for several hours at 250°C in a dynamic vacuum. Molybdenum tubing was obtained from Thermoelectron Corporation, nickel tubing from Tube Sales Co. and the fused silica from laboratory stock.

Synthesis

Crystals of $NdMo_8O_{14}$ were first discovered by P. Gougeon[6] in the product resulting from an attempt to prepare the neodymium analogue of $Ca_{5.45}Mo_{18}O_{32}$[9]. To prepare the pure $NdMo_8O_{14}$ phase, neodymium sesquioxide, molybdenum dioxide and molybdenum powder were mixed in a ratio to make $Nd_{1.2}Mo_8O_{14}$, pressed into a pellet, sealed into an evacuated fused silica tube and heated to 1250°C for one day. The purpose of adding the small excess of Nd_2O_3 was to compensate for a slight reaction of this oxide with the fused silica reaction vessel which becomes frosted during the reaction.

The preparation of analogues of this compound proved to be very challenging. Using the same conditions as stated above, heating a pressed pellet of Sm_2O_3, MoO_2 and Mo powder for one day at 1250°C, the pure compound $SmMo_8O_{14}$ was obtained. However, none of the other rare earth compounds could be obtained as pure compounds by using this technique. In two other cases; *viz.* cerium and gadolinium, the MMo_8O_{14} analogue was observed as a minor component of the product mixture, with other previously known phases making up the bulk of the samples. In most cases, the reaction mixture was contained in a fused silica vessel; however, in the cases of the more basic rare earth oxides (e.g. La_2O_3) the reaction mixture interacted readily with the glass tube, causing devitrification and disintegration of the tube. Thus, all of the reactions which required use of these basic oxides were performed in sealed nickel and molybdenum tubes which were in turn sealed inside fused silica jackets.

Next, experiments were performed where reaction conditions and stoichiometries were varied in order to prepare the pure analogues. Reaction times were increased to periods up to three weeks, temperatures used were in the range from 1000°C to 1500°C, and samples were cooled by both quenching and slow cooling. Chemically, the different approaches included varying the stoichiometry over the range $0.5 < x < 1.5$ in the formula $RE_xMo_8O_{14}$ (RE = rare earth cations), and using different starting

materials, mainly the substitution of rare earth molybdates for the rare earth oxides. By using these processes, the preparation of pure $CeMo_8O_{14}$ was accomplished. For the successful preparation a mixture of cerium dioxide, molybdenum dioxide and molybdenum powder in the ratios of 1:6:2 was pressed into a pellet and sealed in a molybdenum tube. This mixture was then heated to 1285°C for four days to give $CeMo_8O_{14}$. An x-ray powder pattern confirmed that no other crystalline phases were present. All the other lanthanides, with the exception of promethium, were used in an attempt to prepare the $REMo_8O_{14}$ compounds but the products were always some other known phases, not the Mo_8O_{14} analogues.

X-ray Powder Diffraction Data

An Enraf Nonius Delft triple focusing Guinier x-ray powder diffraction camera with Cu Kα radiation (λ = 1.54056 Å) was used to obtain the powder diffraction data. National Bureau of Standards silicon powder was mixed with all samples as an internal standard. Lattice parameters for $NdMo_8O_{14}$, $SmMo_8O_{14}$, $CeMo_8O_{14}$, and $GdMo_8O_{14}$, calculated by using a least squares refinement of d-spacings from Guinier powder patterns, are shown in Table II.1. Powder patterns for the compounds were indexed on the basis of an orthorhombic unit cell. The lattice parameters were calculated using all of

the observed lines in the powder patterns except in the cases of the impure phases, where the lines for other known phases were removed. The observed and calculated d-spacings are given in Tables II.2 through II.5.

Magnetic Susceptibility

The magnetic susceptibility measurements on $NdMo_8O_{14}$ and $CeMo_8O_{14}$ were performed by Won-Choon Lee and Lance Miller in Professor Johnston's group at Iowa State University using ~ 50 mg samples of x-ray pure materials on a Quantum Design SQUID (superconducting quantum interference device) susceptometer. The gram susceptibility as a function of temperature from 4 K to 390 K was provided by these measurements.

Resistivity

A pressed pellet of $NdMo_8O_{14}$, previously sintered at 1200°C, was prepared for the measurements by attaching four Pt-wires with silver epoxy glue. The electrical resistivity measurements were made by using a standard four probe AC (27.5 Hz) method. The cooling rate was approximately one to two degrees per minute, with the temperature readings provided by Pt/Pt-Re

and carbon resistance thermometers. Slight and inconsequential differences in readings occurred as the system was switched between electrodes.

RESULTS AND DISCUSSION

The purpose of this study was to clarify some aspects of the MMo_8O_{14} structure and to learn about the physical properties. A short description of the structure, determined by P. Gougeon, will be followed by a discussion of the physical properties and how those properties relate to the structural parameters.

The compound $NdMo_8O_{14}$ crystallizes in the orthorhombic system, space group Ama2, with the following lattice parameters: a = 9.191(1) Å, b = 9.996(1) Å, and c = 11.121(1) Å. The structure consists of discrete Mo_8 cluster units which may be considered as bicapped octahedra or two butterfly units condensed front to back as shown in Figure II.1. The oxygen atoms in the structure bridge the edges of the cluster unit in the fashion found in the M_6X_{12} arrangement. The ternary cations reside in sites between the Mo_8 units and are coordinated by twelve oxygen atoms in a tetracapped cube, as seen in Figure II.2. Figure II.3 shows the unit cell minus the oxygens and the neodymium atoms. A study of the distances in this compound shows that there is a close intercluster approach of the atoms Mo1 and Mo4 with d(Mo-Mo) = 3.059(2) Å. This distance is much longer than a Mo-Mo single bond, but the calculated Pauling bond order is 0.18, which appears to be significant. By using a simple assessment of the metal cluster electron count based on the

valence of elements in the formula unit, one finds that there are 23 electrons per Mo_8 unit. In this case it appears that there is an odd number of electrons in the system. This odd number of cluster electrons presents two opportunities to determine if the long intercluster interaction is actually a bonding interaction, namely, the studies of the resistivity and the magnetic susceptibility.

The preparation of the rare earth analogues of $NdMo_8O_{14}$ was more difficult than expected. Since the trivalent rare earth cations are all similar in radius and exhibit similar reactivity, one might expect that under similar conditions this structure could be formed by each member. As stated earlier, the only examples prepared were the cerium, neodymium, samarium, and gadolinium MMo_8O_{14} compounds. Many parameters were varied in the reactions in an attempt to prepare these analogues in pure form. Among these conditions was the use of mixtures of rare earth cations, such as a mixture of lanthanum and luticium or yttrium and luticium. In the former case, the mixed cations would give an average ionic radius similar to that found for neodymium. The latter attempt to make the mixed cation material was motivated by the need to obtain a MMo_8O_{14} species with a nonmagnetic cation. However, in these cases with the mixed cations, no MMo_8O_{14} compounds were observed. While it could be rationalized that the heavier rare earth cations are sufficiently different in radii and reactivity, the two

glaring discrepancies in this series are the praseodymium and europium compounds since they fall within the observed series. The case of europium is perhaps the most easily explained in that it can form the 2+ cation relatively easily and therefore stabilize a different structure type. This is confirmed in the reactions performed here by the observation of the compound $EuMo_5O_8$ in the reaction mixture. The x-ray powder pattern of the product mixture showed a phase which is isomorphous with the compound $SrMo_5O_8$[10]. The case of praseodymium is a little more difficult to explain. The x-ray powder patterns of the product mixtures always showed the formation of $Pr_4Mo_4O_{11}$, an analogue of $Gd_4Mo_4O_{11}$[11], and unreacted molybdenum dioxide, even though the ratio of praseodymium to molybdenum was always 1:4 or less. All of the other rare earths also form the latter phase, but not to the exclusion of the the MMo_8O_{14} phase in the cases of Ce, Nd, Sm, and Gd. Thus it appears that $M_4Mo_4O_{11}$ is not necessarily the thermodynamically favored phase and some other factor must be involved in the lack of formation of MMo_8O_{14} in the praseodymium system.

In the MMo_8O_{14} compounds, one can imagine that if the long intercluster distance is not a bonding interaction, the resistivity should show insulating or semiconducting behavior. The size and morphology of the crystals did not lend themselves to the attachment of electrodes, so it was necessary to use a sintered pressed pellet in the experiment. Only the

$NdMo_8O_{14}$ was tested because of the difficulty in obtaining single phase materials of the other analogues. While the specific resistivity was quite high (646 Ω at 295 K), metallic behavior was indicated by the decreasing resistivity ratio as the temperature decreased, Figure II.4. Evidently the intercluster interactions result in sufficient electron delocalization that a narrow conduction band is formed.

The next type of measurement undertaken was the magnetic susceptibility. Since the method of electron counting from the formula unit gives an odd number of electrons on the cluster unit, one would expect some contribution to the magnetic moment by the unpaired electrons of the clusters if the clusters indeed behave as isolated units. A problem with using the original compound, $NdMo_8O_{14}$, is that the rare earth cation, with it's three *4f* electrons, will contribute a large moment of it's own which might cause a problem in determining the moment arising from the cluster unit. The ideal candidates for this study would be the lanthanum, lutecium, or yttrium analogues, since they have completely filled or completely empty *4f* shells. However, as explained earlier, these analogues, either singly or as mixed cation examples, could not be prepared, therefore the neodymium and cerium analogs were studied.

The magnetic susceptibility data of these compounds were analyzed using a simple Curie - Weiss relationship , especially for the high temperature data (T > 80K). The formula used was as follows:

$$\chi_M = \chi^\circ + C/(T-\theta), \text{ with } C = \mu^2\beta^2N/3k$$

where χ_M = molar susceptibility, T = temperature, θ = Weiss temperature, μ = magnetic moment, N = Avagadro's number, k = Boltzmann's constant and β = Bohr magneton.

The molar susceptibility was obtained by multiplying the gram susceptibility obtained from the measurements by the molecular weight. Figure II.5 and II.6 show the susceptibility of $NdMo_8O_{14}$ and $CeMo_8O_{14}$, respectively. The plots of χ^{-1} vs. T have straight line behavior at higher temperatures, above about 100 K, and in this region they fit the Curie - Weiss law very well. At lower temperatures the experimental curve starts to drop away towards the temperature axis. This agrees with other studies of rare earth oxides[12] and can be explained by the depopulation of thermally excited levels in the ground term created by crystal field affects. Since at ordinary temperatures kT is of the same order as the energy separations produced by the crystal field, this makes the susceptibility simulate the Curie - Weiss law.

By using just the high temperature data and making a least squares fit to the Curie - Weiss equation, the magnetic moments of the compounds were calculated. The values for C, θ, and μ, respectively, are: for $NdMo_8O_{14}$, 1.28(4), -0.11(4)°, and 3.25(5) μ_b; for $CeMo_8O_{14}$, 0.596(6), -29.4(9)°, and 2.2(1) μ_b. It can be seen that the magnetic moments are close to what was expected for the free ions, 3.62 for Nd^{3+} and 2.54 for Ce^{3+} [13]. Since this is the case, we can conclude that the cluster is not contributing at all to the moment. Because electron counting indicates that there should be an odd number of electrons, in the absence of intercluster bonding it would be expected that the cluster would contribute a component from at least one unpaired electron to the total magnetic moment. The measurements indicate that this is not the case and that the clusters must have their spins coupled through intercluster Mo-Mo bonding interactions.

CONCLUSIONS

This study was initially undertaken to determine which of the rare earth elements could form the MMo_8O_{14} structure and if the short intercluster Mo-Mo distance (3.059 Å) found in $NdMo_8O_{14}$ reflected intercluster bonding and was an actual bonding distance or was simply imposed by the crystal structure. The first difficulty encountered involved preparation of the rare

earth analogues of $NdMo_8O_{14}$. Surprisingly, the only members observed were the cerium, samarium, and gadolinium compounds, with only the first two obtained as pure material. In the x-ray powder patterns of the reaction materials, several other molybdenum oxide phases were observed, such as $RE_4Mo_{18}O_{32}$,$RE_4Mo_4O_{11}$ and molybdenum dioxide. This suggests that perhaps these other phases, as well as the starting materials, are more stable in the ranges of composition and temperature in which the studies were carried out. The resistivity and susceptibility data seem to indicate that there is intercluster interaction, and therefore the long intercluster distance of 3.059 Å is indeed a bonding distance, at least in these compounds.

REFERENCES

1 Torardi,C.C; McCarley,R.E.; J.AmChem.Soc, 1979, 101, 3963

2 Lii,K.-H.; McCarley,R.E.; Sangsoo,K.; Jacobson,R.A.; J Solid State Chem. 1986, 64, 347

3 Torardi,C.C; McCarley,R.E.; J. Solid State Chem., 1981, 37, 393

4 Aleandri,L.E.; Ph.D. Dissertation, Iowa State University, Ames, Iowa, 1987, Section 1

5 Mattausch,H.; Simon,A.; Peters,E.-M.; Inorg. Chem., 1986, 25, 3428.

6 Gougeon,P.; McCarley,R.E.; unpublished results, Department of Chemistry, Iowa State University, Ames, Iowa, 1986.

7 Lii,K.-H.; Wang,C.C.; Wang,S.L.; J. Sol. State Chem. 1988, 77, 407

8 Hibble,S.J.; Cheetham,A.K.; Bogle,A.R.L.; Wakerley,H.R.; Cox,D.E.; J. Am. Chem. Soc. 1988, 110, 3295

9 McCarley,R.E.; Lii,K.-H.; Edwards,P.A.; Brough,L.F.; J. Solid State Chem., 1985, 57, 17.

10 Torardi,C.C.; Ph.D. Dissertation, Iowa State University, Ames, Iowa 1981, Section V.

11 Lii,K.-H.; Ph.D. Dissertation, Iowa State University, Ames, Iowa, 1985, Section 6.

12 a.Proc. 4th Conf. Rare Earth Res.; Eyring,L., ed.;
Gordon and Breach, New York, 1964, 93.
b.Penney,W.G.; Phys. Rev., 1933, 43, 485.

13 Ashcroft,W.N.;Mermin,N.D.:"Solid State Physics",Plennum, New York, 1982,657

Table II.1 Lattice parameters of MMo_8O_{14}

Compound	a (Å)	b (Å)	c (Å)	V (Å^3)
$NdMo_8O_{14}$[a]	9.191(1)	9.996(1)	11.121(1)	1021.7(1)
$NdMo_8O_{14}$[b]	9.208(1)	10.004(1)	11.143(1)	1026.4(2)
$CeMo_8O_{14}$[b]	9.209(2)	10.003(3)	11.130(2)	1025.2(4)
$SmMo_8O_{14}$[b]	9.196(8)	9.995(8)	11.130(8)	1023.(1)
$GdMo_8O_{14}$[b]	9.204(3)	9.999(3)	11.132(5)	1024.6(7)

[a]From single crystal structure determination.

[b]From Guinier x-ray powder data.

Table II.2 X-ray powder diffraction data for $NdMo_8O_{14}$

d-spacing		intensities		
observed	calculated	I_{obs}	I_{calc}	hkl
5.79	5.789	s	70	111
5.565	5.571	m	19	002
5.006	5.002	m	14	020
4.610	4.604	w	10	200
3.918	3.916	m	48	211
3.723	3.722	w	9	022
3.542	3.549	w	8	202
3.386	3.387	w	6	220
3.253	3.257	s	71	113
3.015	3.018	vs	82	131
2.894	2.894	vw	6	222
2.837	2.838	vs	100	311
2.777	2.777	s	63	213
2.624	2.625	m	37	231
2.500	2.501	w	6	040
2.434	2.434	m	18	024
2.413	2.414	m	28	140
2.397	2.396	m	25	133
2.352	2.353	s	53	124
2.301	2.302	m	19	400
2.197	2.198	w	13	240
2.185	2.184	m	27	233
2.152	2.152	m	23	224
2.118	2.117	w	9	115
1.966	1.967	m-s	50	215
1.938	1.939	m-s	45	340
1.907	1.907	s	83	324
1.816	1.816	m	30	135
1.810	1.811	m	34	251
1.787	1.788	m	40	511
1.694	1.694	m	4	440
1.719	1.719	w	19	235

Table II.3 X-ray powder diffraction data for $CeMo_8O_{14}$

d-spacing		intensities		
observed	calculated	I_{obs}	I_{calc}	hkl
5.780	5.789	s	70	111
5.550	5.571	m	19	002
4.996	5.002	m	14	020
4.596	4.604	w	10	200
3.253	3.257	s	71	113
3.017	3.018	vs	82	131
2.879	2.894	vw	6	222
2.838	2.838	vs	100	311
2.776	2.777	s	63	213
2.625	2.625	m	37	231
2.502	2.501	w	6	040
2.435	2.434	m	18	024
2.414	2.414	m	28	140
2.397	2.396	m	25	133
2.353	2.353	s	53	124
2.302	2.302	m	19	400
2.199	2.198	w	13	240
2.184	2.184	m	27	233
2.153	2.152	m	23	224
1.966	1.967	m-s	50	215
1.939	1.939	m-s	45	340
1.910	1.907	s	83	324
1.813	1.816	m	30	135
1.788	1.788	m	40	511
1.717	1.719	w	19	235
1.695	1.694	m	27	440
1.672	1.672	m	43	424
1.527	1.528	vvw	9	353
1.483	1.483	m	16	540
1.468	1.469	m-s	63	524
1.430	1.431	m-s	56	064

Table II.4 X-ray powder diffraction data for $SmMo_8O_{14}$

d-spacing		intensities		
observed	calculated	I_{obs}	I_{calc}	hkl
5.778	5.789	s	70	111
5.561	5.571	m	19	002
4.991	5.002	m	14	020
4.595	4.604	w	10	200
3.910	3.916	m	48	211
3.260	3.257	s	71	113
3.011	3.018	vs	82	131
2.832	2.838	vs	100	311
2.776	2.777	s	63	213
2.620	2.625	m	37	231
2.436	2.434	m	18	024
2.412	2.414	m	28	140
2.354	2.353	s	53	124
2.298	2.302	m	19	400
2.196	2.198	w	13	240
2.184	2.184	m	27	233
2.153	2.152	m	23	224
1.968	1.967	m-s	50	215
1.937	1.939	m-s	45	340
1.906	1.907	s	83	324
1.818	1.816	m	30	135
1.810	1.811	m	34	251
1.784	1.788	m	40	511
1.692	1.694	m	27	440
1.672	1.672	m	43	424
1.480	1.483	m	16	540
1.468	1.469	m-s	63	524
1.431	1.431	m-s	56	064

Table II.5 X-ray powder diffraction data for $GdMo_8O_{14}$

d-spacing		intensities		
observed	calculated	I_{obs}	I_{calc}	hkl
5.781	5.789	s	70	111
5.001	5.002	m	14	020
3.919	3.916	m	48	211
3.542	3.549	w	8	202
3.255	3.257	s	71	113
3.018	3.018	vs	82	131
2.875	2.894	vw	6	222
2.836	2.838	vs	100	311
2.775	2.777	s	63	213
2.624	2.625	m	37	231
2.432	2.434	m	18	024
2.413	2.414	m	28	140
2.392	2.396	m	25	133
2.351	2.353	s	53	124
2.300	2.302	m	19	400
2.195	2.198	w	13	240
2.183	2.184	m	27	233
2.151	2.152	m	23	224
1.966	1.967	m-s	50	215
1.937	1.939	m-s	45	340
1.906	1.907	s	83	324
1.812	1.811	m	34	251
1.787	1.788	m	40	511
1.719	1.719	w	19	235
1.694	1.694	m	27	440
1.672	1.672	m	43	424
1.482	1.483	m	16	540
1.468	1.469	m-s	63	524

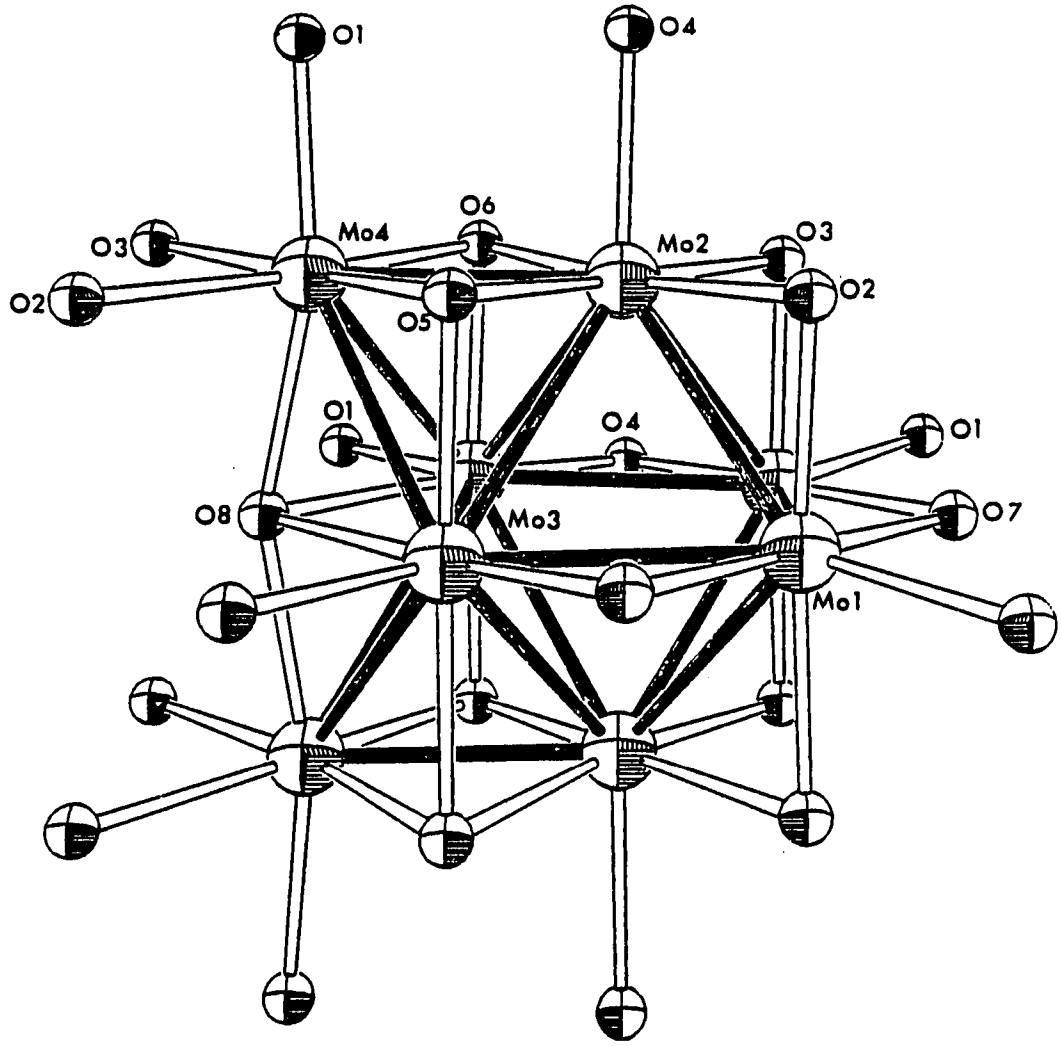

Figure II.1 An ORTEP drawing of the Mo_8O_{14} cluster unit from the compound $NdMo_8O_{14}$

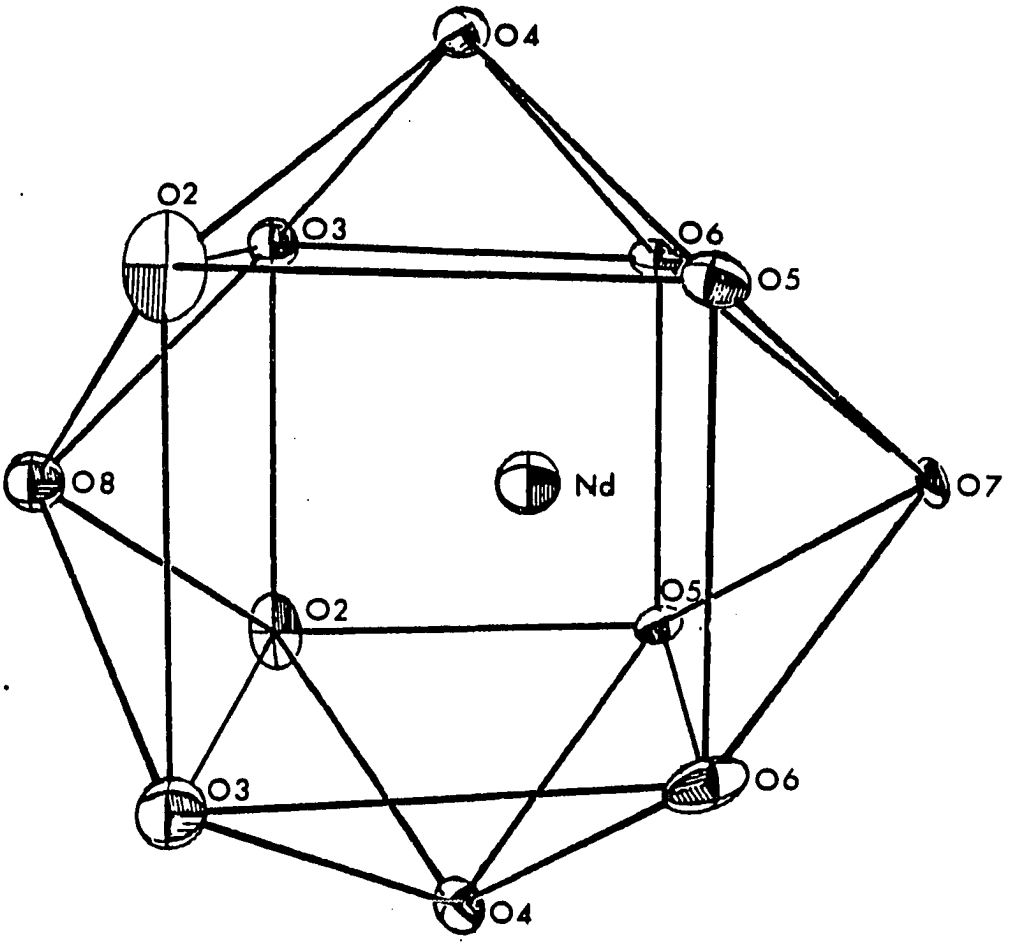

Figure II.2 **A polyhedral representation of the coordination around the neodymium atoms in $NdMo_8O_{14}$**

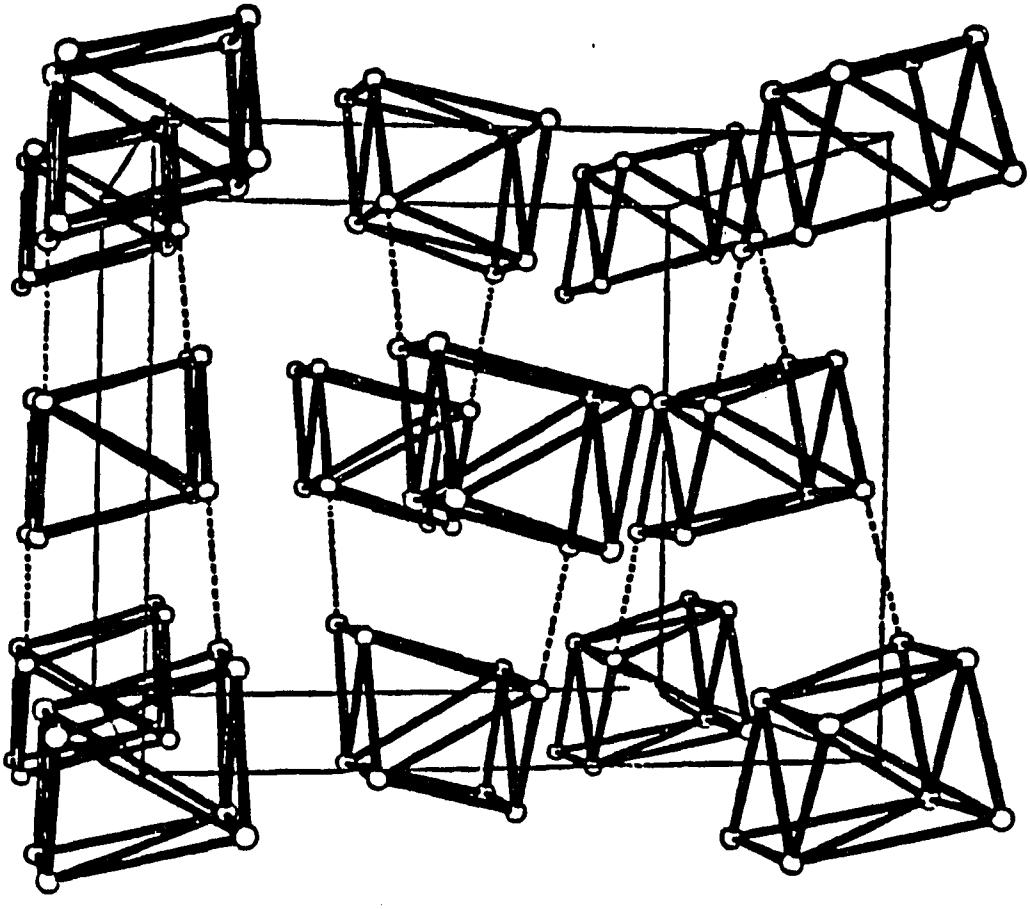

Figure II.3 An ORTEP drawing of the unit cell for $NdMo_8O_{14}$. The oxygen and neodymium atoms have been omitted for clarity. The dashed lines indicate the shortest intercluster Mo-Mo distance

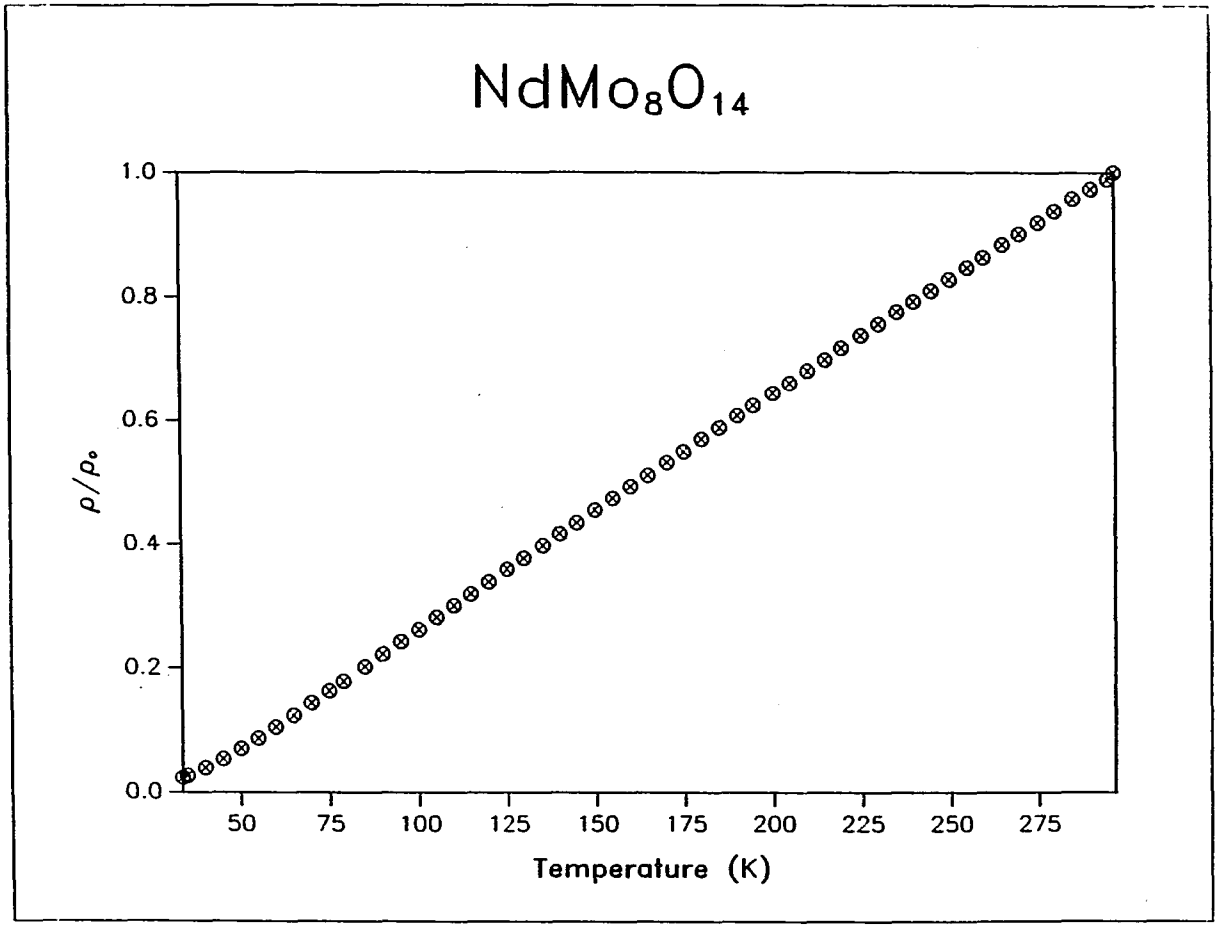

Figure II.4 **The resistivity ratio, ρ(T)/ρ(295), versus temperature curve for $NdMo_8O_{14}$**

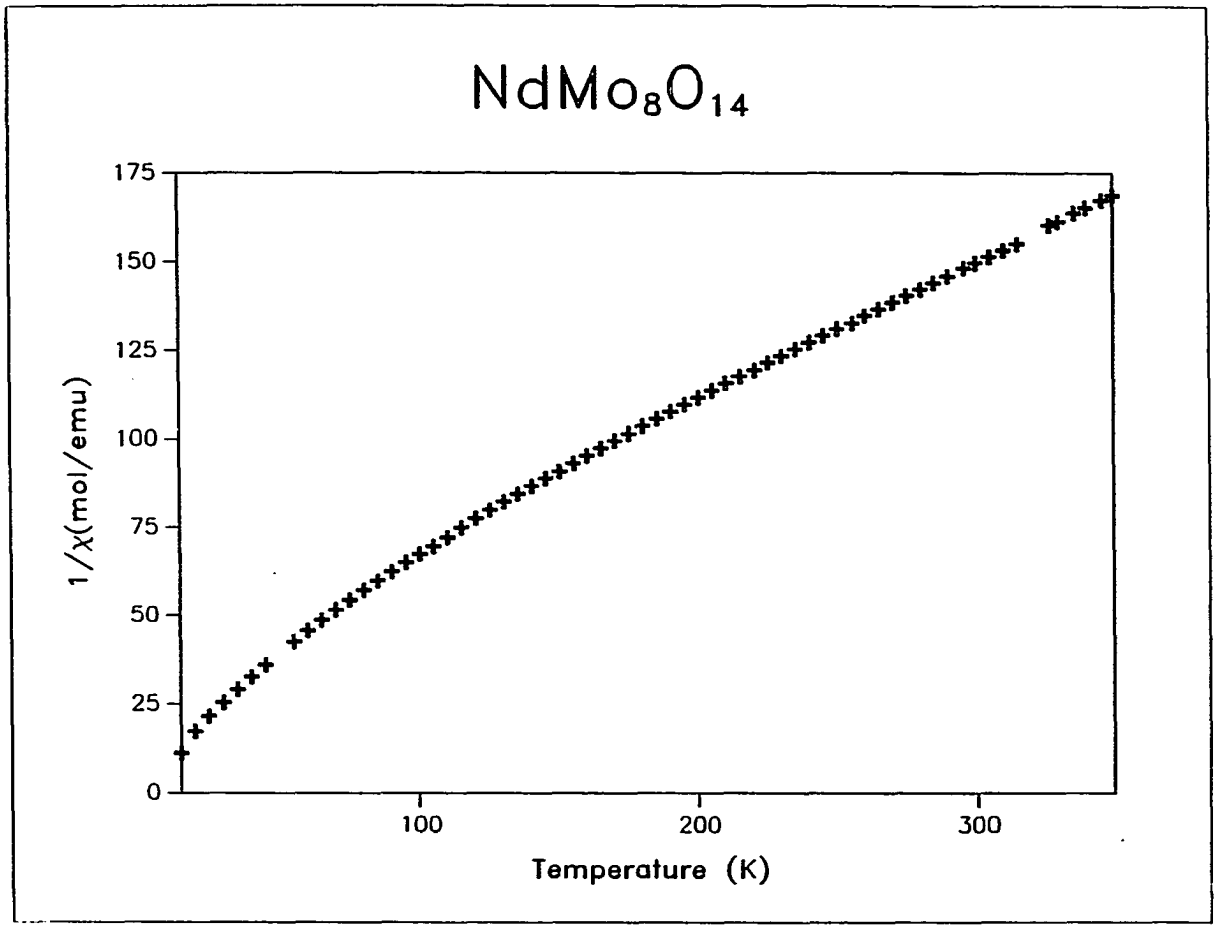

Figure II.5 **The reciprocal magnetic susceptibility versus temperature curve for $NdMo_8O_{14}$**

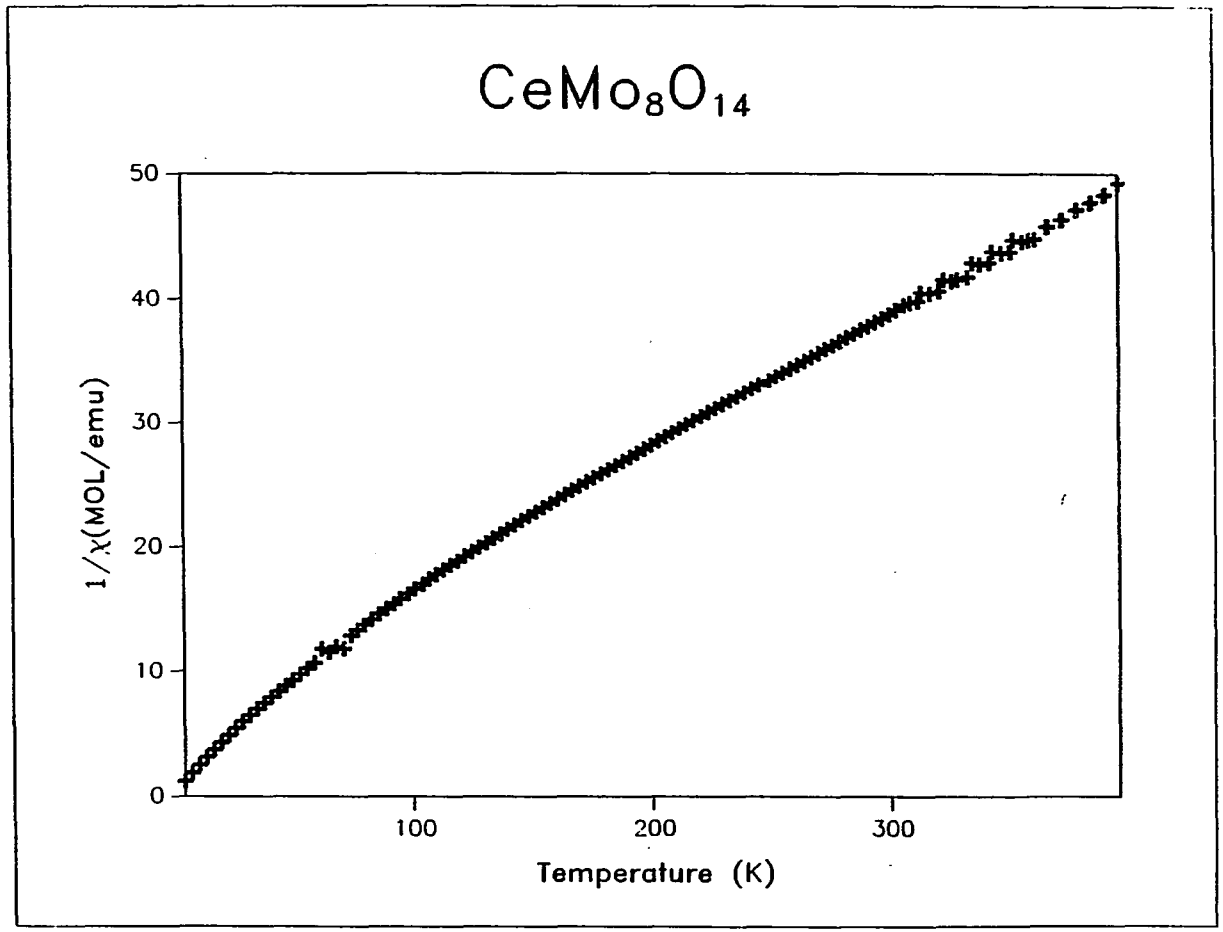

Figure II.6 **The reciprocal magnetic susceptibility versus temperature curve for $CeMo_8O_{14}$**

Section III

PREPARATION OF A MOLYBDENUM INTERMETALLIC COMPOUND: $Ni_xFe_{7-x}Mo_6$

INTRODUCTION

Novel and interesting compounds are often found in reactions designed to prepare completely different products. This was the case in the preparation of the intermetallic compound $Ni_xFe_{7-x}Mo_6$. This compound was observed in a reaction designed to prepare a reduced molybdenum oxide. The phase, designated as the μ-phase, was first observed by Arnfelt and Westgren[1] as the compound Fe_7W_6. A number of studies on various binary and ternary systems of either tungsten or molybdenum at around approximately 1200°C have shown a region in the phase diagram where the μ-phase exists at high tungsten and molybdenum weight ratios[2].

A great deal of study has been performed on these systems because they have been observed in some austenitic steels at grain boundaries. This phase at the grain boundaries causes the steel to become very brittle and is therefore undesirable in a large number of cases. The studies have been largely performed by Japanese steel companies and reported in the patent literature.

A more recent example of the formation of the μ-phase was found in the attempt to prepare suitable starting materials for making cobalt/tungsten carbide composite materials[3]. In this preparation, a cobalt tungstate and tungsten trioxide mixture was reduced in a hydrogen atmosphere at 800° to

1100°C. The x-ray powder pattern of the products showed that Co_7W_6 was present and accounted for up to 50% of the product, depending on the conditions.

A crystal structure of the Co - Mo μ-phase was obtained in 1962 by Forsyth and d'Alte da Veiga on a twinned crystal[4]. The compound was prepared by melting a pressed compact of Mo and Co powders in a vacuum pressure of 10^{-5} mm Hg; twinned crystals were found growing off of the compact. The researchers found that the compound crystallized in the space group $R\bar{3}m$ with the lattice constants of a = 4.762(1) Å and c = 25.615(1) Å, and the structure was refined to a final R-factor of 6.5%.

This section will describe the preparation of non-twinned crystals and the subsequent crystal structure of the ternary μ-phase compound $Ni_xFe_{7-x}Mo_6$.

MATERIALS AND METHODS

The molybdenum powder (Aldrich Gold Label 99.99%) was dried under a dynamic vacuum at 250°C as was the molybdenum dioxide (Alfa products). Neodymium(III)oxide, fired at 900°C in air to remove volatile constituents, was obtained from the Ames Laboratory Materials Preparation Center. The nickel (Fisher Scientific) and iron (J. T. Baker) were used as obtained. The fused silica tubing was from laboratory stock.

Synthesis

The compound was first observed as crystals in an attempted preparation of $NdMo_8O_{14}$. In the reaction, the amount of MoO_2 used was approximately one-half that needed to prepare the MMo_8O_{14} phase. The reaction mixture, 2:12:7 of Nd_2O_3:MoO_2:Mo, was mixed intimately, placed as a loose powder into a fused silica jacket sealed under vacuum and heated to 1250°C. After three days the tube was rapidly cooled to room temperature and hexagonal plate-like crystals were observed in what had been the cool end of the tube, which had been kept at about 1200°C. This proved to be the compound $Ni_xFe_{7-x}Mo_6$ which was later synthesized as the pure phase (x = 2.5) using a pressed pellet of the metal powders and heating to 1200°C. This

Ni-Fe-Mo phase was also found as crystals in attempts to make analogues of $Gd_4Mo_4O_{11}$[5].

Single Crystal X-ray Structure Analysis

A black, hexagonal plate with dimensions 0.08mm x 0.08mm x 0.01mm, isolated from the reaction described above, was used for the film work and subsequent structure determination. From the oscillation and Weissenberg photographs, the following rhombohedral lattice parameters were obtained, a = 8.90 Å and $\alpha = 30°$. X-ray data collection was accomplished with an Enraf Nonius CAD4 four circle diffractometer. Indexing of the cell was performed on 25 reflections taken from film coordinates and a rhombohedral cell having cell dimensions of a = 4.768(1) Å, c = 25.6559(1) Å in the hexagonal setting was determined. Axial photographs agreed with the above cell. The data showed a reflection condition of -h+k+l = 3n and the Laue symmetry appeared to be 3m so the possible space groups were R32, R3m, and $R\bar{3}m$. A structure solution in the highest symmetry group, namely $R\bar{3}m$, was tried first because the results of a statistical analysis given by the SHELXS 86 direct methods program[6] indicated a centric system. The details of the data collection and refinement are shown in Table III.1.

The direct methods solution (SHELXS 86) showed only five different atomic positions. These positions could all be filled with metal atoms (at first thought to be neodymium and molybdenum) in a layered arrangement, as was expected from the crystal morphology. However, because of the short interlayer distances, there was no room for any oxygen atoms in between the layers. The R factor for the structure was down to 10% at this time. At this point energy dispersive x-ray analysis (EDX), used to ascertain the composition of the crystals, showed that the only elements present were molybdenum, nickel and iron. Molybdenum atoms were then entered into the the three positions with the greatest electron density. The two remaining sites were filled with a mixture of nickel and iron, the multipliers being varied such that the sum of the nickel and iron multipliers would equal the occupancy of the sites. Refinement of positional parameters and anisotropic thermal parameters was performed on the molybdenum atoms while positional parameters, isotropic thermal parameters and multipliers were refined on the mixed nickel/iron sites. Anisotropic thermal parameters were not refined on the nickel/iron sites because the two different atoms on the site caused some difficulty in successful operation of the program. The refinement converged at R = 3.4% and R_w = 4.5%. Tables III.2 and III.3 show the atomic positional and isotropic equivalent thermal parameters, and

the anisotropic thermal parameters are given in Table III.4. Selected interatomic distances are shown in Table III.5.

Energy Dispersive X-ray Analysis

The energy dispersive x-ray analysis (EDX) was performed using a KEVEX Quantum x-ray detector in connection with a JEOL 840A scanning electron microscope at the Materials Analysis Research Laboratory of the ISU Engineering Research Institute. This device was chosen for elemental analysis because of the particle size (single crystals) and the need for detection of oxygen; all elements with an atomic number greater than four could be detected. EDX analysis of the hexagonal plates from the original reaction showed that the only elements present were nickel, iron and molybdenum. Quantitatively, the experiment showed the weight percentages of these elements to be Ni - 19.5% , Fe - 23.3% and Mo - 57.0% giving a formula of $Ni_{3.35}Fe_{4.21}Mo_6$.

DESCRIPTION OF THE STRUCTURE

Figure III.1 shows the rhombohedral cell of this compound with 13 atoms in the unit cell. It can be seen that all of the positions except for Ni/Fe2 lie

on the body diagonal (111) forming long chains of closely spaced metal atoms. The order of these chains is six molybdenum atoms which are separated by a nickel/iron site. The other Ni/Fe site forms a triangle just off the body diagonal at almost the same height along the body diagonal as the Ni/Fe1 atoms.

A better overall view of the structure can be obtained using the hexagonal setting, Figures III.2 and III.3. The structure has a layered structure as was expected from the crystal morphology (plate behavior) and is made up of so called Kagomé nets[7], see Figure III.4. The Kagomé nets are made up of atoms with a designated symmetry of 3.6.3.6. which describes the geometric shapes around each point in the lattice. This means that around each atom are a triangle, a hexagon, a triangle and a hexagon in that order. Another way of looking at the Kagomé nets is that they are a hexagonal closest packed layer with every alternate row occupied 50% of the time. These Kagomé layers, made up of Ni/Fe2 atoms, are stacked in a AABBCC arrangement. In between the layers of the same type (AA for example) there are three layers of molybdenum atoms, composed of two layers of Mo2 sites and one layer of Mo1 sites. In between different layers, which are translated by 1/3 2/3 2/3 and 2/3 1/3 1/3 in the unit cell, there are also three layers consisting of two layers of Mo3 sites and one layer of Ni/Fe1 sites on an inversion center.

Table III.5 gives the coordination number of each atom and important distances in the structure. Figure III.5 shows the coordination around a Mo1 atom. The Mo1 atom is coordinated to three other Mo1 atoms in virtually the same plane (a pseudo mirror plane) with three Mo2 atoms above and below the plane and three Ni/Fe2 atoms (triangles in the Kagomé net) above and below that. This gives the Mo1 site a coordination number of fifteen inside a regular polyhedron. Figure III.6 shows the coordination around the Mo2 atoms. This atom is not coordinated to any other atoms in the same layer but is directly above a hexagon of Mo1 atoms and directly below a hexagon of Ni/Fe2 atoms (from the Kagomé net). Each of the hexagons is capped, the Mo1 hexagon by another Mo2 atom and the Ni/Fe2 hexagon by a Mo3 atom. This gives the Mo2 site a coordination number of fourteen in a regular polyhedron. The Mo3 atoms have the highest coordination number in this structure, and can be seen in Figure III.7. Below the site are three layers of equilateral triangles, the closest made up of Ni/Fe1 atoms with the sides of the triangle 4.768 Å in length (the a-axis cell length). The next layer down is made up of Mo3 atoms in the same configuration as the previous layer but rotated 60°. The third triangle, made up of Ni/Fe2 atoms, is smaller, 2.400 Å on a side, and again rotated by 60°. Above the Mo3 site is a hexagon of Ni/Fe2 atoms which is capped by a Mo2 atom. This gives the Mo3 atoms a coordination number of sixteen.

The Ni/Fe1 atoms, seen in Figure III.8, are the most symmetric since they lie on an inversion center. In the layer below the atoms there is a equilateral triangle of Mo3 atoms (4.768 Å on a side) and below that is a smaller triangle of Ni/Fe2 atoms (2.400 Å on a side) rotated by 60°. The inversion center gives the same arrangement of atoms above the Ni/Fe1 site, giving the site a coordination number of twelve in a perfect dodecahedral arrangement. The final atom, NiFe/2, is also coordinated in a dodecahedron but is slightly distorted, see Figure III.9. Since the atoms in the Kagomé net are so closely packed, each atom in the net has a close approach to four other atoms. Above and below the atoms are coordinated to two molybdenum atoms, Mo3 above and Mo2 below. In the next layer below are two more atoms, rotated 90° from the previous pair, which are Mo1 atoms. Finally, above the site are one Ni/Fe 1 atom and one Mo3 atom which are in layers close enough together that they make up the final two atoms.

DISCUSSION

This structure type has been seen in a number of molybdenum and tungsten systems such as the cobalt and iron species of both metals as well as in a number of ternary systems[2]. The isothermal phase diagram of the Ni-Fe-Mo system[2b] with the so called μ phase in the region around 45% Mo,

between 0% and 20% Fe, and between 55% and 25% Ni is shown in Figure III.5. The diagram shows that the μ-phase is stable over a large range of nickel and iron compositions but from the results of the refinement on the multipliers of the positions, it appears that the nickel tends to prefer the Ni/Fe1 site(the Kagomé net sites), with the nicklel atom occupation of these sites at 57%, while the iron atoms prefer the Ni/Fe2 sites with an occupation of 69%, giving a stoichiometry of $Ni_{2.43}Fe_{4.57}Mo_6$. It could be that a composition close to this stoichiometry is the most favorable for the crystal growth through the vapor phase, or the composition is controlled by the relative amounts of nickel and iron impurities in the starting materials. An interesting feature is the close approach of the metal atoms even with the fairly large coordination numbers.

An interesting aspect of the synthesis is the fact that oxygen was present in the system and two of the metals, iron and nickel, were present in impurity amounts. The amount of oxygen present was not sufficient to oxidize the intermetallic but an oxygen species was probably instrumental in the transport of the compound to the cool end of the tube. While it may not be practical on a large scale, the use of oxygen species as transport agents could assist in the formation of pure single crystals of other intermetallic compounds.

REFERENCES

1. Arnfelt,A.; Westgren,A.; Jernkontorets Ann. 1935, 119,185.

2. a. Koester,W.; Tonn,W.; Arch. Eisenhuttenwesen, 1932, 5, 627.
   b. Das,D.K.; Rideout,S.P.; Beck,P.A.; J. Metals, 1952, 191, 1071
   c. Das,D.K.; Rideout,S.P.; Beck,P.A.; J. Metals, 1952, 191, 872
   d. Hengler,F.; Kohsok,H.; Rev. Met., 1949, 46, 569

3. French,G.J.; Sale,F.R.; J. Mater. Sci., 1985, 20, 1291

4. Forsyth,J.B.; d'Alte da Veiga,L.M.; Acta Crystallogr., 1962, 15, 543.

5. Hsiao,M.-W.; McCarley,R.E.; Unpublished results, Chemistry Department, Iowa State University, Ames, Iowa, 1987.

6. Sheldrick,G.M.; Institut fur Anorganische Chemie der Universitat Gotting, F.R.G

7. Frank,F.C.; Kasper,J.S.; Acta Cryst., 1958, 11, 184

Table III.1 Crystallographic data for $Ni_xFe_{7-x}Mo_6$

Crystal system: Trigonal Space group: $R\bar{3}m$ (no.166)
Hexagonal lattice parameters:
a = 4.768(1) Å c = 25.6559(1) Å V = 505.1(1) Å Z = 3
Trigonal lattice parameters:
a = 8.984(1) Å α = 30.78(1)° V = 168.4(1) Å Z = 1
crystal dimensions: 0.08mm x 0.08mm x 0.01mm
absorption coefficient: 115.1 cm^{-1}
calculated density: 4.500 g cm^{-3}
Reflections used for absorption correction:
$02\bar{2}$, 030, $04\bar{4}$, $04\bar{1}$
Diffractometer: Enraf Nonius CAD4
Radiation: Mo Kα (λ = 0.70926 Å)
Monochrometer: graphite
Collection temperature: 25°C
Scan type: $\omega/2\theta$
Scan half width: 0.85 + 0.34tanθ
Standard reflections:
monitered 3
frequency measured every 250 reflections
intensity variation none
Reflections measured: HKL, $H\bar{K}L$
Maximum 2θ: 55°
Nonredundant reflections collected: 181
observed [I>3σ(I)]: 145
Number of parameters refined: 16
R (%)[a]: 3.4
R_w (%)[b]: 4.5

---

[a] $R = \Sigma||F_o| - |F_c|| / \Sigma|F_o|$.
[b] $R_w = [\Sigma\omega(|F_o| - |F_c|)^2 / \Sigma\omega|F_o|^2]^{1/2}$.

Table III.2 Positional parameters for $Ni_xFe_{7-x}Mo_6$

Hexagonal Cell

atom	Position[a]	x	y	z	multiplier	B_{eq}
Mo1	c (3m)	0.0	0.0	0.33463(8)	1/6	0.11(4)
Mo2	c (3m)	0.0	0.0	0.04763(8)	1/6	0.14(4)
Mo3	c (3m)	0.0	0.0	0.15127(8)	1/6	0.19(4)
Ni1	b ($\bar{3}$ m)	1/3	2/3	1/6	0.0467(1)[b]	0.3(1)
Fe1	b ($\bar{3}$ m)	1/3	2/3	1/6	0.0357(1)[b]	0.3(1)
Ni2	h (m)	0.5011(2)	1.0023(4)	0.09011(7)	0.156(1)[c]	0.10(6)
Fe2	h (m)	0.5011(2)	1.0023(4)	0.09011(7)	0.344(1)[c]	0.10(6)

[a] Wyckoff notation in the R$\bar{3}$ m space group.

[b] Sum of the multipliers for the atoms on this site equals 1/12 for full occupation.

[c] Sum of the multipliers for the atoms on this site equals 1/12 for full occupation.

Table III.3 Positional parameters for $Ni_xFe_{7-x}Mo_6$

Trigonal Cell

atom	Position[a]	x	y	z	multiplier	B_{eq}
Mo1	c (3m)	0.33463(8)	0.33463	0.33463(8)	1/6	0.11(4)
Mo2	c(3m)	0.04763(8)	0.04763	0.04763(8)	1/6	0.14(4)
Mo3	c(3m)	0.15127(8)	0.15127	0.15127(8)	1/6	0.19(4)
Ni1	b ($\bar{3}$ m)	1/2	1/2	1/2	0.0467(1)[b]	0.3(1)
Fe1	b ($\bar{3}$ m)	1/2	1/2	1/2	0.0357(1)[b]	0.3(1)
Ni2	h (m)	0.59121	0.59121	0.08781	0.156(1)[c]	0.10(6)
Fe2	h (m)	0.59121	0.59121	0.08781	0.344(1)[c]	0.10(6)

[a] Wyckoff notation in the R$\bar{3}$ m space group.

[b] Sum of the multipliers for the atoms on this site equals 1/12 for full occupation.

[c] Sum of the multipliers for the atoms on this site equals 1/12 for full occupation.

Table III.4 Anisotropic thermal parameters[a] for $Ni_xFe_{7-x}Mo_6$

atom	B_{11}	B_{22}	B_{33}	B_{12}	B_{13}	B_{23}
Mo1	0.11(6)	0.11(6)	0.12(8)	0.05(3)	0	0
Mo2	0.14(6)	0.14(6)	0.15(8)	0.07(3)	0	0
Mo3	0.22(6)	0.22(6)	0.14(8)	0.11(3)	0	0

[a] The general thermal parameter expression used was:

$\exp[1/4(B_{11}h^2a^{*2} + B_{22}k^2b^{*2} + B_{33}l^2c^{*2} + B_{12}hka^*b^* + B_{13}hla^*c^* + B_{23}klb^*c_*)]$.

Table III.5 Interatomic distances (Å) in $Ni_xFe_{7-x}Mo_6$

atom	CN[a]	neighbors	distances
Mo1	15	3Mo1	2.750(3)
		6Mo2	3.0119(8)
		6Ni/Fe2	2.695(2)
Mo2	14	6Mo1	3.0119(8)
		1Mo2	2.444(3)
		1Mo3	2.65898(8)
		6Ni/Fe2	2.621(2)
Mo3	16	1Mo2	2.65898(8)
		3Mo3	2.8632(8)
		3Ni/Fe1	2.7809(3)
		6Ni/Fe2	2.725(3)
		3Ni/Fe2	2.855(2)
Ni/Fe1	12	6Mo3	2.7809(3)
		6Ni/Fe2	2.404(2)
Ni/Fe2	12	1Mo1	2.686(2)
		1Mo1	2.695(2)
		2Mo2	2.621(2)
		1Mo3	2.725(3)
		2Mo3	2.855(3)
		1Ni/Fe1	2.404(2)
		4Ni/Fe2	2.400(2)

[a] CN = coordination number including all atoms at distances within 3.1 Å.

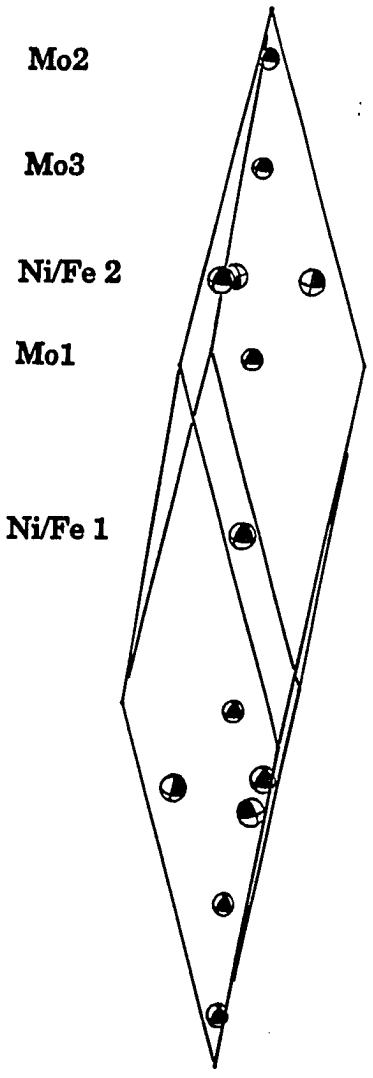

Figure III.1 An ORTEP diagram of the trigonal unit cell for $Ni_xFe_{7-x}Mo_6$

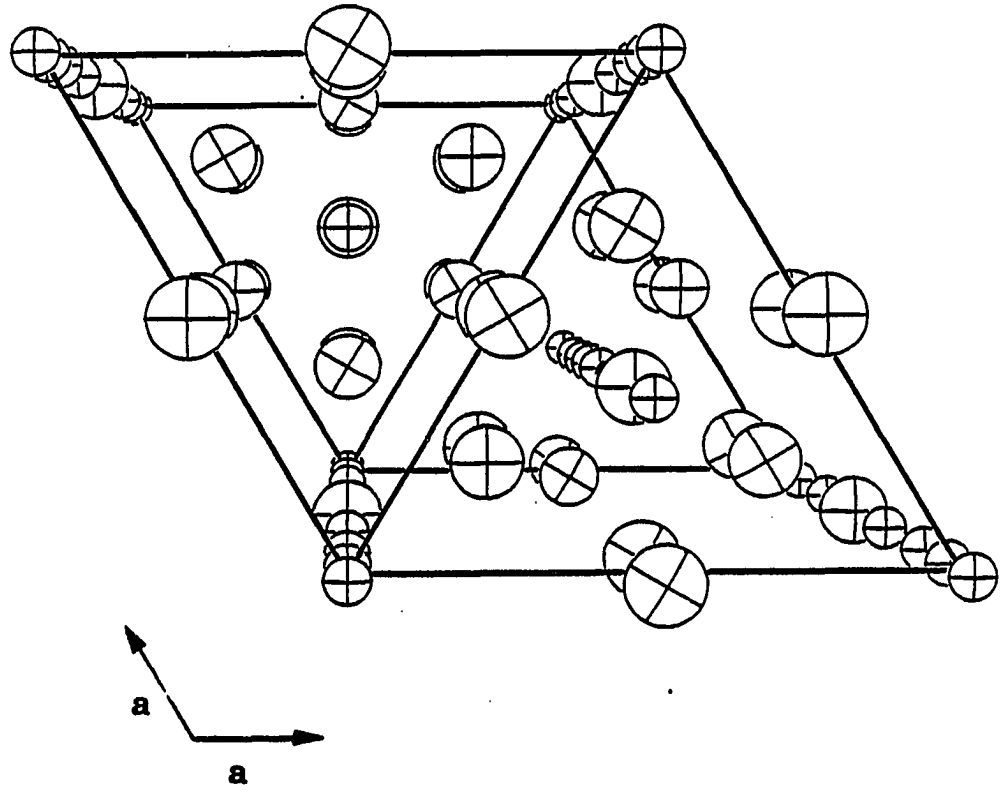

Figure III.2 An ORTEP diagram of the hexagonal unit cell for $Ni_xFe_{7-x}Mo_6$ viewed down the c-axis. All atoms are represented by their 50% thermal ellipsoids. The large ellipsoids represent Ni/Fe atoms and the small ellipsoids represent Mo atoms

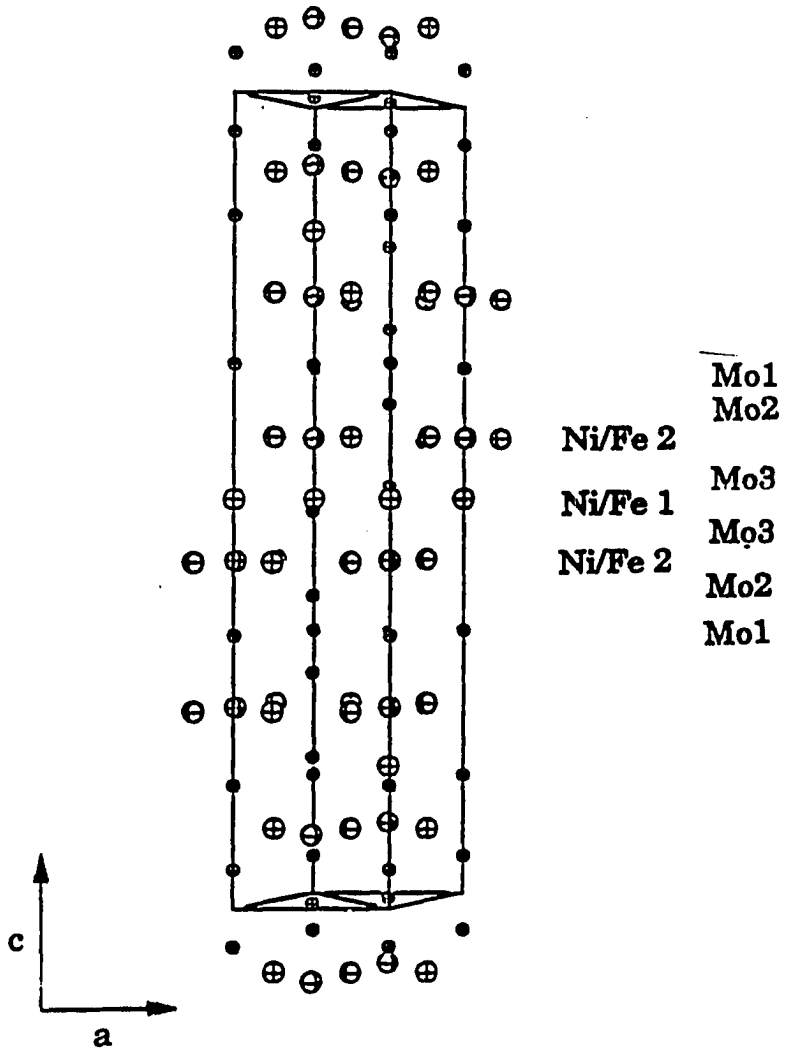

Figure III.3 An ORTEP diagram of the hexagonal unit cell for $Ni_xFe_{7-x}Mo_6$ viewed perpendicular to the c-axis

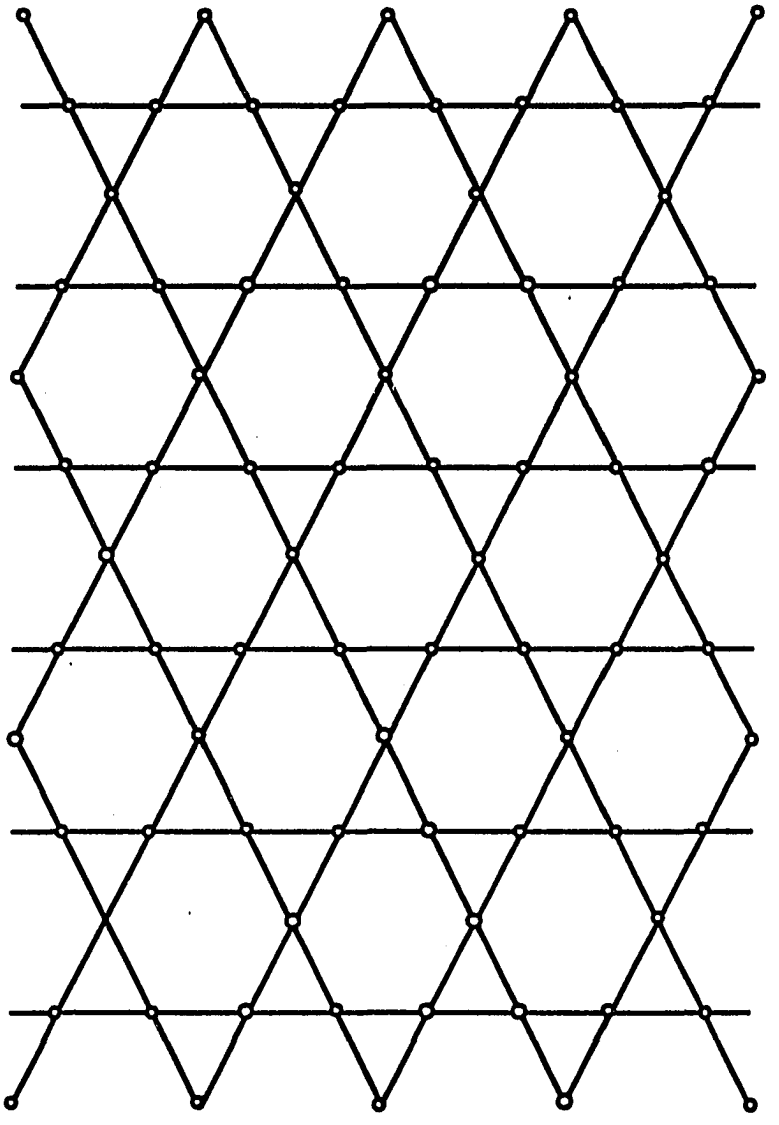

Figure III.4 A drawing of a Kagomè net as viewed down the hexagonal c-axis. Each vertex shown as a small circle represents a Ni/Fe2 atom in the layers found in $Ni_xFe_{7-x}Mo_6$

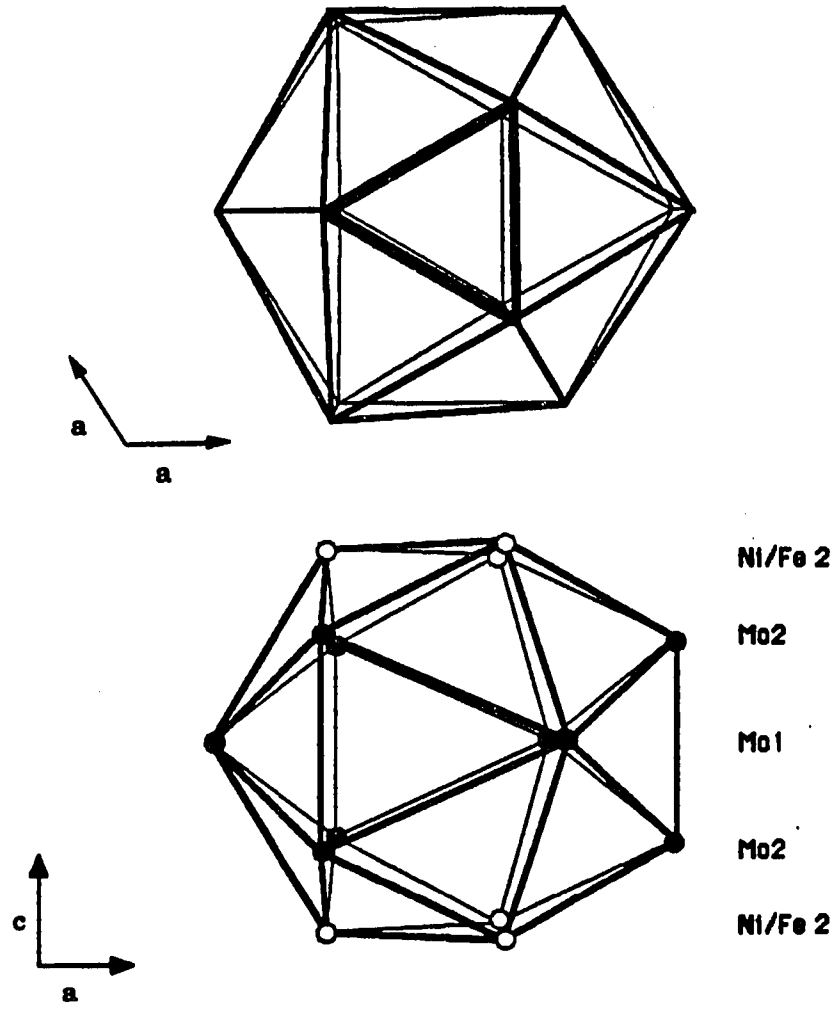

Figure III.5 The coordination sphere around the Mo1 atoms in $Ni_xFe_{7-x}Mo_6$. The Mo1 atom located at the center of the polyhedron is not shown

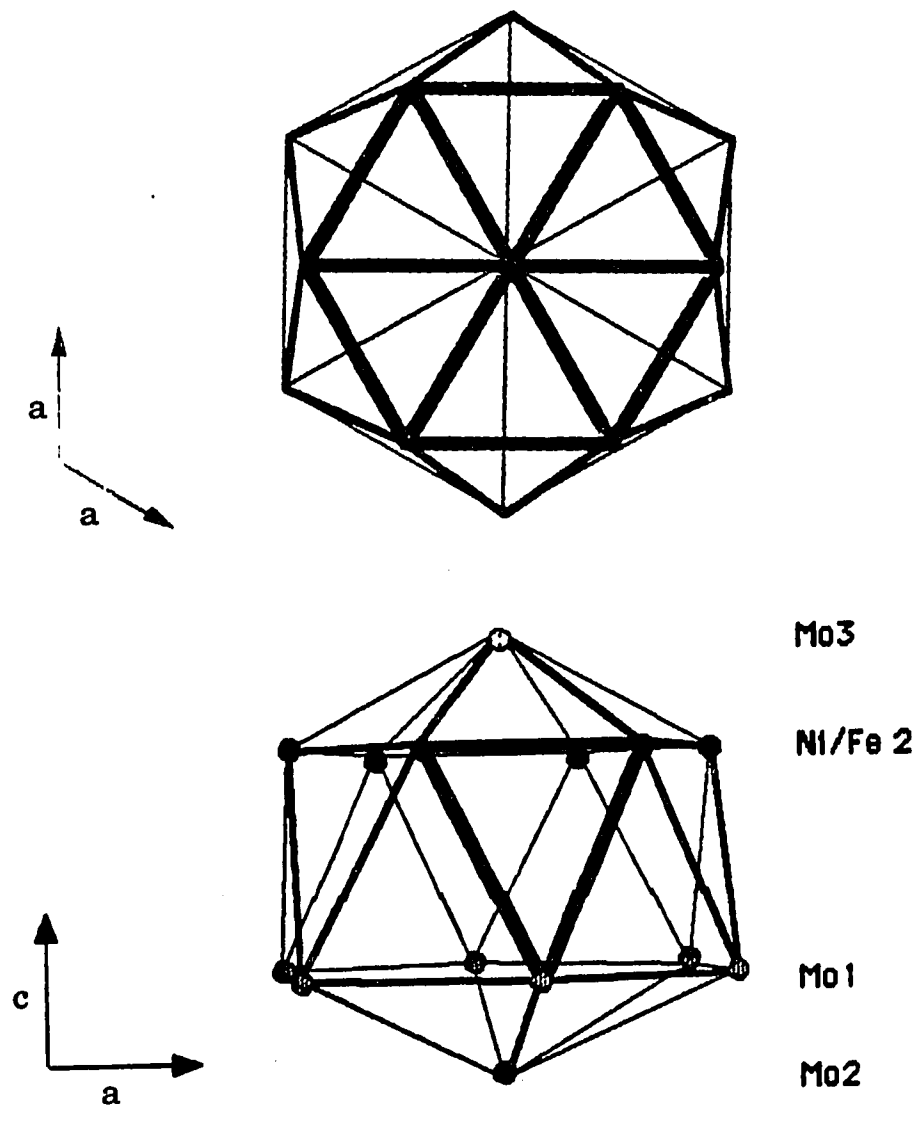

Figure III.6 The coordination sphere around the Mo2 atoms in $Ni_xFe_{7-x}Mo_6$. The Mo2 atom located at the center of the polyhedron is not shown

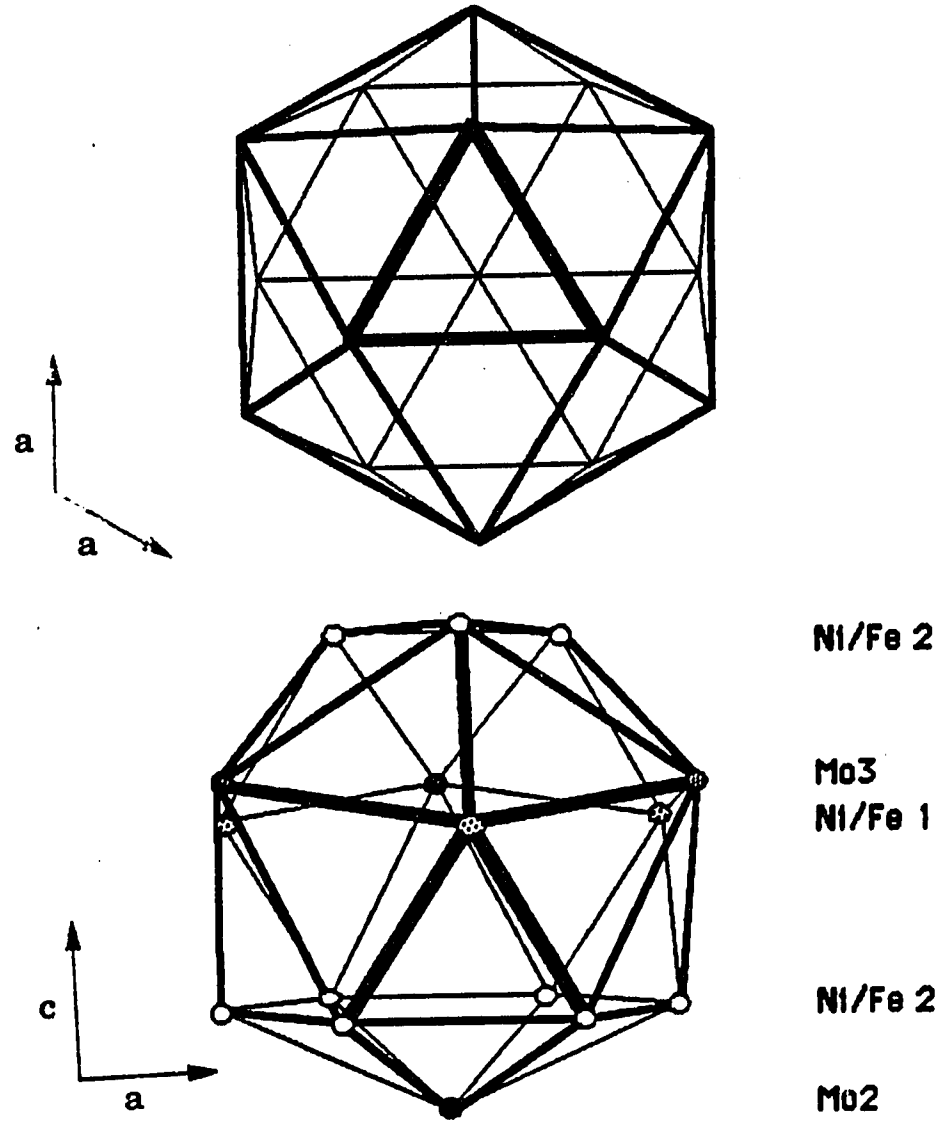

Figure III.7 The coordination sphere around the Mo3 atoms in $Ni_xFe_{7-x}Mo_6$. The Mo3 atom located at the center of the polyhedron is not shown

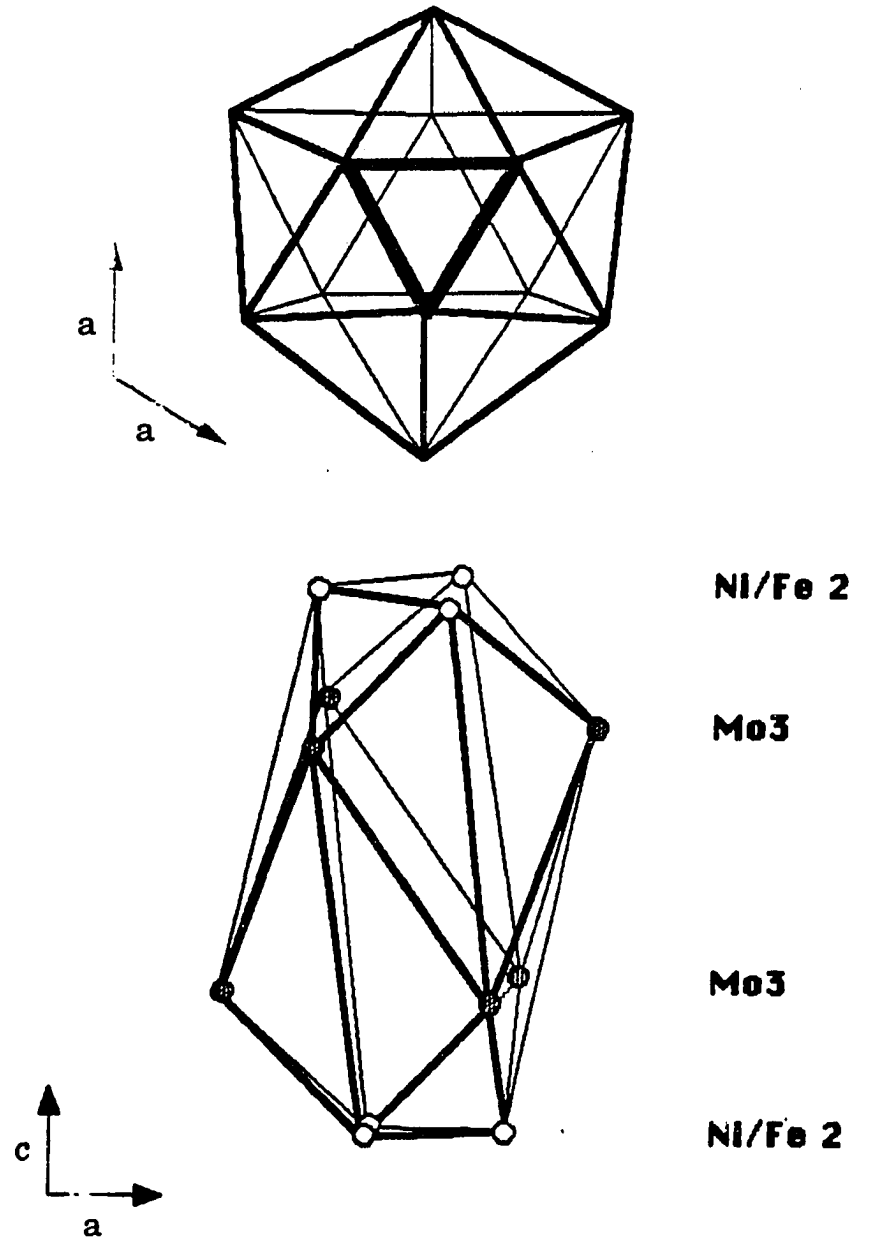

Figure III.8 The coordination sphere around the Ni/Fe1 atoms in $Ni_xFe_{7-x}Mo_6$. The Ni/Fe1 atom located at the center of the polyhedron is not shown

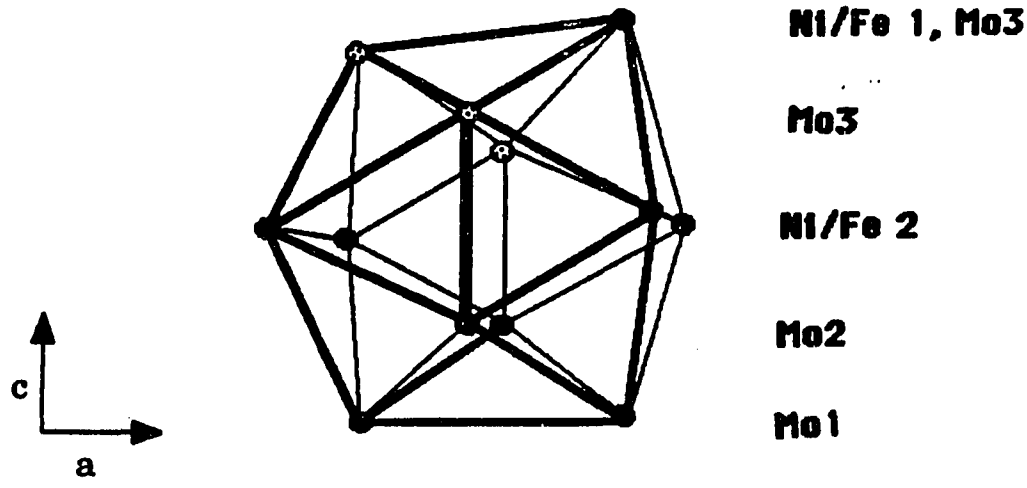

Figure III.9 The coordination sphere around the Ni/Fe2 atoms in $Ni_xFe_{7-x}Mo_6$. The Ni/Fe2 atom located at the center of the polyhedron is not shown

Figure III.10 The isothermal phase diagram for the Ni-Fe-Mo system at 1200°C

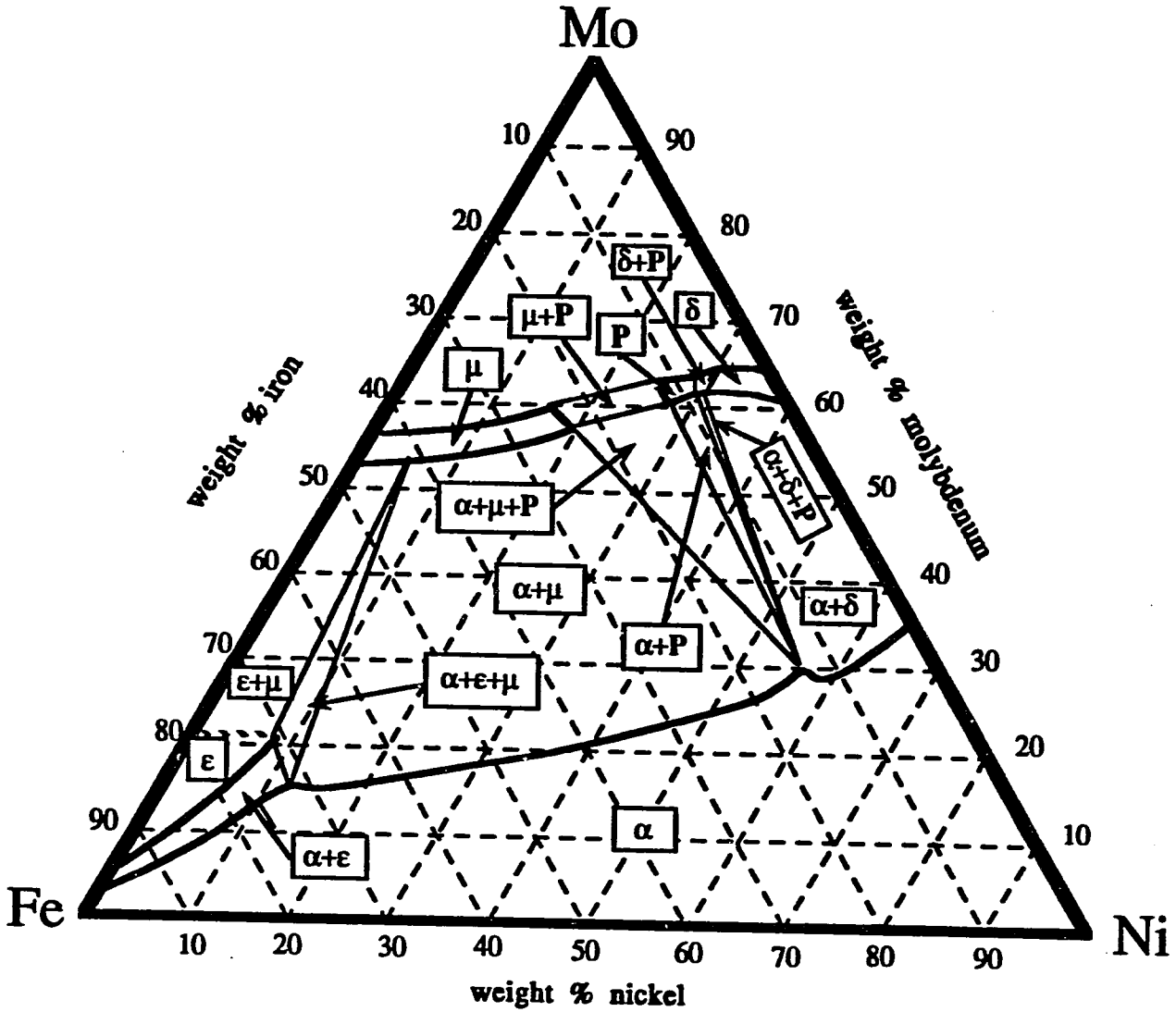
Mo
Fe
Ni
weight % iron
weight % molybdenum
weight % nickel
10
20
30
40
50
60
70
80
90
δ+P
μ+P
P
δ
μ
α+δ+P
α+μ+P
α+μ
α+P
α+δ
ε+μ
α+ε+μ
ε
α
α+ε

REFERENCES

1 a) Yih,S.W.H.; Wang,C.T.; "Tungsten: Sources, Metallurgy, Properties, and Applications", Plenum Press, New York, 1979.
b) Swift,R.A. ed.; "Research of Chrome-Moly Steels" American Society of Mechanical Engineers, New York, 1984.

2 Deaton,J.C.; Solomon,E.I.; Durfor,C.N.; Wetherbee,P.J.; Burgess,B.K.; Jacobs,D.B.; Biochem. Biophys. Res. Commun. 1984, 121, 1042.

3 Chisholm,M.H.; Clark,D.L.; Hampden-Smith,M.J.; Hoffman,D.H.; Angew. Chem Int. Ed. Eng. 1989, 28, 432.

4 Mazdiyasui,K.S.; Cer. Int. 1982, 8, 42.

5 Torardi,C.C.; McCarley,R.E.; J. Am. Chem. Soc. 1979, 101, 3963.

6 McCarley,R.E.; ACS Symp. Ser. 1983, 211, 273.

7 Lii,K.-H.; McCarley,R.E.; Sangsoo,K.; Jacobson,R.A.; J. Sol. State Chem. 1986, 64, 347.

8 Lii,K.-H.; Ph.D. Dissertation, Iowa State University, Ames, Iowa, 1985, Section 6.

9 Torardi,C.C; Calabrese,J.C.; Inorg. Chem. 1984, 23, 3281.

10 Lii,K.-H.; Ph.D. Dissertation, Iowa State University, Ames, Iowa, 1985, Section 5.

11 Aleandri,L.E; Ph.D. Dissertation, Iowa State University, Ames, Iowa, 1987,Section 1.

12 Mattausch,H.; Simon,A.; Inorg. Chem. 1986, 25, 3428.

13 Lii,K.-H.; Wang,C.C.; Wang,S.L.; J. Sol. State Chem. 1988, 77, 407.

14 Hibble,S.J.; Cheetham,A.K.; Bogle,A.R.L.; Wakerley,H.R.; Cox,D.E.; J. Am. Chem. Soc. 1988, 110, 3295.

ACKNOWLEDGEMENTS

I would like to express my appreciation to Professor Robert E. McCarley for his guidance, patience, and support during my years at Iowa State. I would also like to thank all of the professors and staff members at ISU and Ames Lab who assisted me with the various physical measurements reported in this dissertation and with other more mundane pursuits. A great deal of thanks goes to the many people that I have encountered and called friend throughout my stay here. In particular, I would like to recognize Thomas Hendrixson, my crystal guru; Timothy Blatchford, for his many insightful discussions and his friendship; Steve Laughlin, a friend in need is a friend indeed; Ingrid Burgeson, for helping me through these last few months; and to my fellow group members, from whom I learned a great deal and with whom I had a great deal of fun. I would like to give a special thanks to Lori Aleandri whose friendship and support helped me in many troubled times.

Finally, I would like to acknowledge my parents, Roy and Vivian, and the rest of my family. Their support and encouragement made it all seem worthwhile.

This work was supported by the Department of Energy (report IS-T-1381) under contract 7405-eng-82.

quæ nocent, docent